Am J Nucl Med Mol Imaging 2015;5(5):431-456
www.ajnmmi.us /ISSN:2160-8407/ajnmmi0012959

Review Article

Monitoring of anti-cancer treatment with ^{18}F-FDG and ^{18}F-FLT PET: a comprehensive review of pre-clinical studies

Mette Munk Jensen, Andreas Kjaer

Department of Clinical Physiology, Nuclear Medicine & PET and Cluster for Molecular Imaging, Rigshospitalet and University of Copenhagen, Denmark

Received July 16, 2015; Accepted September 10, 2015; Epub October 12, 2015; Published October 15, 2015

Abstract: Functional imaging of solid tumors with positron emission tomography (PET) imaging is an evolving field with continuous development of new PET tracers and discovery of new applications for already implemented PET tracers. During treatment of cancer patients, a general challenge is to measure treatment effect early in a treatment course and by that to stratify patients into responders and non-responders. With 2-deoxy-2-[^{18}F]fluoro-D-glucose (^{18}F-FDG) and 3'-deoxy-3'-[^{18}F]fluorothymidine(^{18}F-FLT) two of the cancer hallmarks, altered energy metabolism and increased cell proliferation, can be visualized and quantified non-invasively by PET. With ^{18}F-FDG and ^{18}F-FLT PET changes in energy metabolism and cell proliferation can thereby be determined after initiation of cancer treatment in both clinical and pre-clinical studies in order to predict, at an early time-point, treatment response. It is hypothesized that decreases in glycolysis and cell proliferation may occur in tumors that are sensitive to the applied cancer therapeutics and that tumors that are resistant to treatment will show unchanged glucose metabolism and cell proliferation. Whether ^{18}F-FDG and/or ^{18}F-FLT PET can be used for prediction of treatment response has been analyzed in many studies both following treatment with conventional chemotherapeutic agents but also following treatment with different targeted therapies, e.g. monoclonal antibodies and small molecules inhibitors. The results from these studies have been most variable; in some studies early changes in ^{18}F-FDG and ^{18}F-FLT uptake predicted later tumor regression whereas in other studies no change in tracer uptake was observed despite the treatment being effective. The present review gives an overview of pre-clinical studies that have used ^{18}F-FDG and/or ^{18}F-FLT PET for response monitoring of cancer therapeutics.

Keywords: ^{18}F-FDG, ^{18}F-FLT, PET, drug development, cancer, response monitoring, tyrosine kinase inhibitors, mTOR inhibitors, anti-angiogenic therapy, chemotherapy, targeted therapy

Introduction

During treatment of cancer patients a general challenge is to measure treatment effect early in a treatment course and by that to stratify patients into responders and non-responders. An advantage for non-responding patients is that shift to other therapies may be done early in the treatment course thereby avoiding unnecessary side-effects of inefficient treatment. However, this requires reliable biomarkers that can accurately predict the treatment outcome. The amount of patients responding to chemotherapy is in many cases 30% or less, this being both to conventional cytotoxic therapy and new targeted therapies [1-4]. Response monitoring has therefore become increasingly important as it can allow for individualized tailored therapy.

Functional imaging of solid tumors with positron emission tomography (PET) imaging is an evolving field with the continuous development of new PET tracers and new applications for existing PET tracers [5]. Two of the cancer hallmarks, altered energy metabolism and increased cell proliferation, can be visualized non-invasively with the widely used PET tracers 2-deoxy-2-[^{18}F]fluoro-D-glucose (^{18}F-FDG) and 3'-deoxy-3'-[^{18}F]fluorothymidine (^{18}F-FLT) [6-8].

It is hypothesized that decreases in glycolysis and cell proliferation may occur in tumors that are sensitive to the applied anti-cancer treat-

ment and that tumors resistant to treatment will show unchanged glucose metabolism and cell proliferation. Furthermore, changes in physiological processes, e.g. metabolic or proliferative pathways are expected to precede morphological changes and changes in growth rate of the tumor. ^{18}F-FDG and ^{18}F-FLT have therefore, both in pre-clinical and clinical studies, been evaluated as imaging biomarkers that can predict and assess responses to various types of anti-cancer therapies including conventional chemotherapeutic drugs and newer targeted anti-cancer therapies in various tumor types. Accordingly, ^{18}F-FDG PET has the potential to facilitate and accelerate drug development by shortening phase II and III using ^{18}F-FDG PET as a surrogate for clinical outcome [9]. Pre-clinical studies in mice with human tumor xenografts may help to predict the expected ^{18}F-FDG and ^{18}F-FLT outcome for specific therapies in later clinical studies.

In this review we therefore present a comprehensive overview of pre-clinical studies that have used either ^{18}F-FDG and/or ^{18}F-FLT PET for response monitoring of cancer therapeutics.

PET imaging

PET is an imaging technique that allows for non-invasive functional imaging in living subjects and dependent on which PET tracer is used different molecular and cellular processes can be visualized without acquiring invasive biopsies. The most widely used PET tracer is the glucose analogue ^{18}F-FDG and in oncology ^{18}F-FDG PET is applied for tumor diagnosis, staging and monitoring of cancer as well as for monitoring of residual disease after completion of a treatment course [9]. ^{18}F-FLT is a widely studied tracer for assessment of cell proliferation [8, 10]. ^{18}F-FDG PET is most often positive at a baseline scan of human solid tumors, whereas a wide range of tumor avidities is observed for ^{18}F-FLT [11, 12].

The change in tumor size after treatment is often used as a surrogate marker of survival in clinical studies, as for many cancer types, tumor shrinkage has been correlated with overall survival [1, 13]. In clinical studies treatment monitoring can be performed using the Response Evaluation Criteria In Solid Tumors (RECIST) [14]. The RECIST criteria are based on anatomical tumor burden measured by computed tomography (CT). In 2009, an updated version of the RECIST guideline, RECIST 1.1, was published. In RECIST 1.1, ^{18}F-FDG PET measurements have been incorporated; however, only as an adjunct to determination of progression by identification of new lesions. The new guideline includes comments on the possibility for future use of PET for treatment evaluation in clinical trials when the technique becomes more standardized and widespread available [14]. Furthermore, in 2009, a guideline proposing the use of ^{18}F-FDG PET for tumor response assessment termed PET Response Criteria In Solid Tumors (PERCIST) was published. The PERCIST guideline proposes the use of ^{18}F-FDG PET for tumor response assessment [4]. In this guideline it is argued that treatment can be effective despite minimal changes in tumor size which is a concern especially during treatment with cytostatic therapies.

^{18}F-FDG-PET

In the 1970s the first whole-body ^{18}F-FDG PET was acquired and ^{18}F-FDG PET has subsequently become widely available and is frequently used in cancer diagnostics, staging and monitoring of recurrent and residual disease after completion of a treatment course [9]. ^{18}F-FDG is a glucose analogue where the 2-carbon hydroxyl group has been substituted with an ^{18}F isotope. Like glucose, ^{18}F-FDG is taken up in cells by the glucose transporters (GLUT) and thereafter phosphorylated by hexokinases (HK) [15]. Further metabolism of ^{18}F-FDG is prevented due to lack of the 2-carbon hydroxyl group and the phosphorylated ^{18}F-FDG is trapped in the cells (**Figure 1**) [16]. The requirements of glucose are higher due to increased glycolysis in cancer cells compared to normal cells, a phenomenon known as the Warburg effect, and high expression of glucose transporters as well as hexokinases are characteristics of many cancers [9, 17].

^{18}F-FLT-PET

^{18}F-FLT, a thymidine analogue labeled with an ^{18}F isotope, was introduced in 1998 by Shields et al. [18]. ^{18}F-FLT PET is used to study cell proliferation *in vivo* [18, 19]. ^{18}F-FLT is incorporated into cells by the pyrimidine salvage pathway paralleled with thymidine. After phosphorylation by thymidine kinase 1 (TK1) ^{18}F-FLT is trapped intracellular; however, the phosphory-

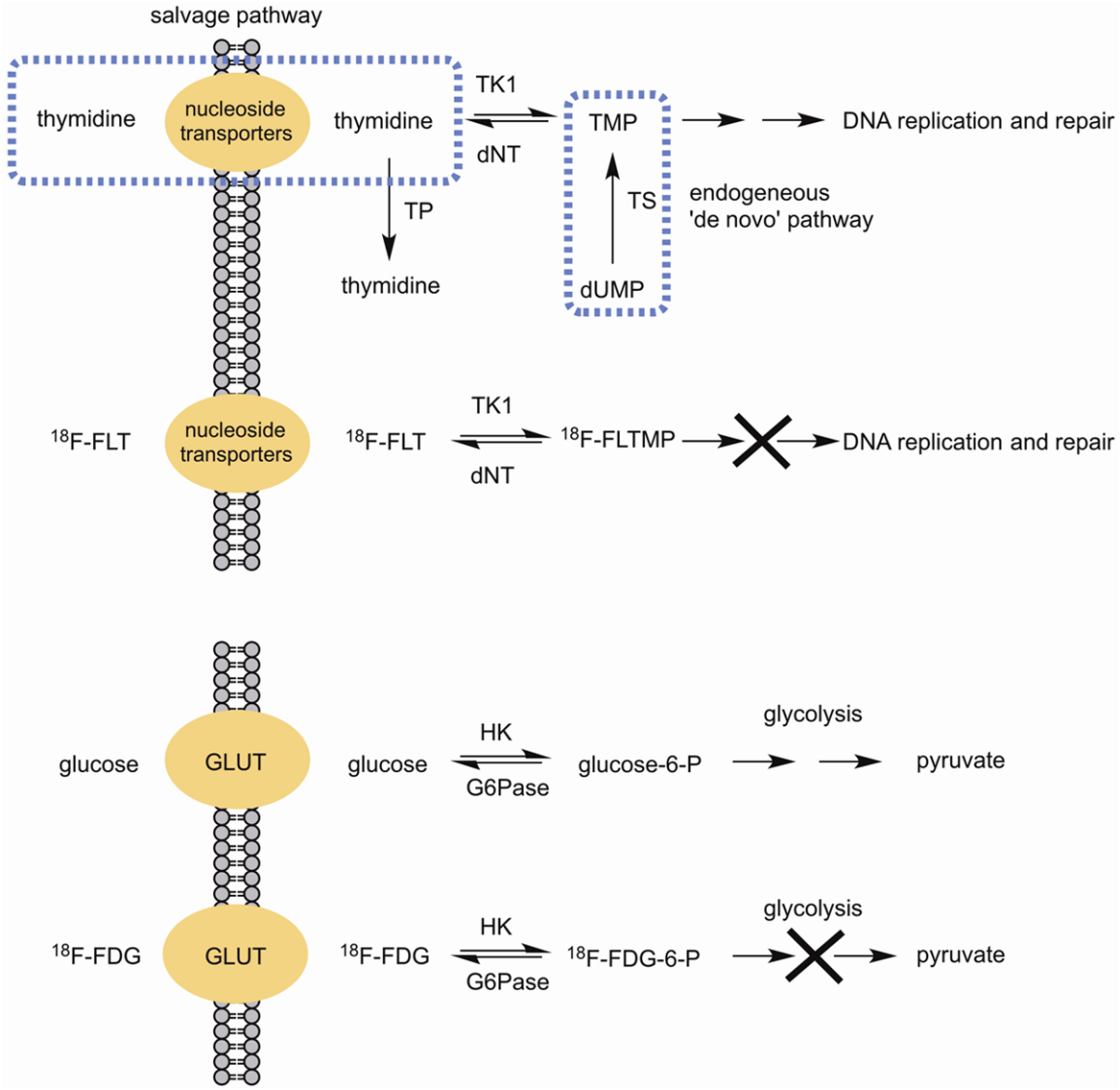

Figure 1. ^{18}F-FLT and ^{18}F-FDG uptake mechanism. ^{18}F-FLT enters the cell through nucleoside transporters by the salvage pathway paralleled with thymidine. ^{18}F-FDG enters the cells paralleled with glucose. ^{18}F-FLT - 3'-deoxy-3'-[^{18}F] fluorothymidine; ^{18}F-FLTMP - ^{18}F-FLT-monophosphate; TK1 - thymidine kinase 1; dNT - 5'(3')-deoxyribonucleotidase; TMP - thymidine monophosphate; TS - thymidylate synthase; dUMP - deoxyuridine monophosphate; TP - thymidine phosphorylase; ^{18}F-FDG - 2-deoxy-2-[^{18}F] fluoro-D-glucose; HK - hexokinase; glucose-6-P - glucose-6-phosphate; G6Pase - glucose-6-phosphatase.

lated ^{18}F-FLT is not incorporated into DNA (**Figure 1**) [20]. TK1 is mainly expressed during the S-phase of cell cycle [21, 22]. ^{18}F-FLT uptake has shown to be positively correlated with cell growth and TK1 activity [21, 23] and several studies have shown a positive correlation between ^{18}F-FLT uptake and tumor cell proliferation measured by Ki67 protein expression [10, 24-33]. The tracer uptake into cells is mediated by equilibrative nucleoside transporters (ENT) 1 and 2 and concentrative nucleoside transporters (CNT) 1 and 3 [34-36]. ^{18}F-FLT uptake gives consequently a measure of the uptake and incorporation of thymidine into DNA and therefore the tracer uptake does not give a direct measure of cell proliferation but is a surrogate marker of the proliferative status of cells. The ratio of the salvage pathway versus the *de novo* synthesis of thymidine to fulfill the cancer cells demand for thymidine will determine baseline ^{18}F-FLT uptake in a tumor. In cancer cells mainly relying on *de novo*

Table 1. ^{18}F-FDG PET of tyrosine kinase inhibitor therapy

Target	Drug	Reference	Tumor placement	Cell line and origin	Treatments	Scan time (days after treatment initiation)	Results	Same paper comparison with ^{18}F-FLT
EGFR	erlotinib	[38]	sc	PC9, HCC827 and H1975 human lung adenocarcinoma	daily	2 and 4	→	+
	erlotonib	[41]	sc	CAL33 and CAL166 human head and neck carcinoma	one dose	1 and 3	↓↓	-
	gefitinib	[37]	sc	H3255, HCC4006, A549 and H1975 NSCLC and A431 human epithelial carcinoma	two doses	2	↓↓	-
HER2	trastuzumab	[46]	sc	syngenic MMTV/HER2 mammary, BT474 human breast cancer	twice weekly/3 weeks	1 weekly	→	+
	trastuzumab	[47]	sc	MDA-MB-361 and MDA-MB-231 human breast cancer	once weekly/3 weeks	2, 9 and 16	↓ (day 16)	-
Pan-HER	afatinib	[49]	sc	N87 human gastric cancer	daily/21 days	7, 14 and 21	→	-
	canertinib (CI-1033)	[48]	sc	A431 human squamous cell carcinoma	daily	3 and 7	↓↓	+
	PKI-166	[30]	sc	A431 human squamous cell carcinoma	daily	7, 14 and 21	↓↓	+
c-KIT	imatinib	[50]	sc	FDC-P1 murine hemopoietic cell line	twice daily	4 h and day 1 and 2	↓↓	-
	imatinib	[51]	sc	GIST882 gastrointestinal stromal cell line	twice daily	1 and 8	↓↓ (day 1)	-
c-MET	rilotumumab	[54]	sc	U87MG human glioblastoma	twice weekly/1 week	1, 2, 3, 4, and 7	↓↓	+
	CE-355621	[57]	sc	U87MG human glioblastoma	one dose	1, 3, 7 and 9	↓	-
	crizotinib	[55]	sc	U87MG human glioblastoma and GTL-16 human gastric cancer	daily	2, 5, 7 and 13	↓↓ (day 13 GTL-16) → (U87MG)	+
	BAY 853474	[56]	sc	Hs746T human gastric cancer	twice daily	2 and 4	↓	+

sc: subcutaneous; NSCLC: non-small cell lung cancer; →: no change in ^{18}F-FDG uptake; ↓↓: decrease in ^{18}F-FDG uptake compared with baseline; ↓: decreases in ^{18}F-FDG uptake compared with a control group; ↑↑: increases in ^{18}F-FDG uptake compared with baseline; ↑: increases in ^{18}F-FDG uptake compared with a control group. If both treatment sensitive and treatment resistant tumor models were analyzed, only the ^{18}F-FDG results from the tumor sensitive cell lines were included in the result column.

Table 2. ^{18}F-FLT PET of tyrosine kinase inhibitor therapy

Target	Drug	Reference	Tumor placement	Cell line and origin	Treatments	Scan time (days after treatment initiation	Results	Same paper comparison with ^{18}F-FDG
EGFR	erlotinib	[38]	sc	PC9, HCC827 and H1975 human lung adenocarcinoma	daily	2 and 4	↓↓	+
	erlotinib	[39]	sc	A431 human squamous cell carcinoma	daily/4 days	3	↓↓	-
	erlotinib	[40]	sc	HCC827, H1975 and H1650 human NSCLC	daily	3	↓↓	-
	cetuximab	[39]	sc	SCC-1 human squamous cell carcinoma	every 3 days	6	↓↓	-
	cetuximab	[44]	sc	H1975 human NSCLC	one dose	3	↓↓	-
	cetuximab	[45]	sc	DiFi and HCT-116 human colorectal carcinoma	3 doses/week	7	→	-
	CL-387, 785	[40]	sc	H1975 human NSCLC	daily	3	↓↓	-
	WZ4002	[40]	sc	H1975 human NSCLC	daily	3	↓↓	-
HER2	trastuzumab	[46]	sc	syngenic MMTV/HER2 mammary cancer, BT474 human breast cancer	twice weekly/3 weeks	1 weekly	↓↓	+
Pan-HER	CI-1033	[48]	sc	A431 human squamous cell carcinoma	daily	3 and 6	↓↓	+
	PKI-166	[30]	sc	A431 human squamous cell carcinoma	daily	6 h and day 1, 2, 7, 14 and 21	→ (6 h, day 1) ↓↓ (day 2, 7, 14 and 21)	+
c-MET	rilotumumab	[54]	sc	U87MG human glioblastoma	twice weekly/1 week	1, 2, 3, 4 and 7	↓↓ (from day 4)	+
	crizotinib	[55]	sc	U87MG human glioblastoma and GTL-16 human gastric cancer	daily	2, 4/5 and 7/8	↓↓ (day 4 and 7 GTL-16 and day 8 U87MG)	+
	BAY 853474	[56]	sc	Hs746T human gastric cancer	twice daily	2 and 4	↓	+

sc: subcutaneous; NSCLC: non-small cell lung cancer; →: no change in ^{18}F-FLT uptake; ↓↓: decrease in ^{18}F-FLT uptake compared with baseline; ↓: decreases in ^{18}F-FLT uptake compared with a control group; ↑↑: increases in ^{18}F-FLT uptake compared with baseline; ↑: increases in ^{18}F-FLT uptake compared with a control group. If both treatment sensitive and treatment resistant tumor models were analyzed, only the ^{18}F-FLT results from the tumor sensitive cell lines were included in the result column.

Table 3. ^{18}F-FDG PET of PI3K/AKT/mTOR inhibitor therapy

Target	Drug	Reference	Tumor placement	Cell line and origin	Treatments	Scan time (days after treatment initiation)	Results	Same paper comparison with ^{18}F-FLT
mTOR	everolimus	[59]	sc	SUDHL-1 and Karpas299 human lymphoma	daily/14 days	5	→	+
	everolimus	[67]	sc	NCI-N87 human gastric cancer	daily	1, 2, 8 and 15	↓↓	-
	everolimus	[66]	Lymph node metastasis (B16/BL6) sc (H596, HCT116, KB13)	B16/BL6 murine melanoma, H596 human lung carcinoma, HCT116 human colorectal carcinoma and KB13 human cervical cancer	daily	2/3 and 6/7	↓↓ (B16/BL6 and H596) → (HCT116 and KB13)	+
	everolimus	[68]	sc	H727 human carcinoid cancer	daily	1, 3 and 10	→	+
	rapamycin	[65]		U87MG and LN-299 human malignant glioblastoma	one dose	2	↓↓	+
	temsirolimus	[63]	sc	Daudi human B-lymphoblast	NA	2, 4, 7, 9 and 14	↓↓	+
	temsirolimus	[62]	sc	Daudi human B-lymphoblast	NA	2, 4, 7, 9 and 14	↓↓	-
	temsirolimus	[64]	sc	Granta-519 human mantle cell lymphoma	NA	1, 2, 4, 7, 9, 11 and 14	↓↓ (day 1 and 2)	+
	temsirolimus	[60]	sc	ACHN human renal cell adenocarcinoma	twice daily	1	↓↓	-
	AZD8055	[58]	sc	U87MG human glioblastoma	daily	1 h and day 4	↓	+
AKT	AZD5363	[69]	sc	U87MG human glioblastoma, BT474C human breast cancer and Calu-6 human lung cancer	daily	4 h, day 4 (U87MG) day 3 (all models)	↓ (4 h) U87MG ↓↓ (day 4) U87MG ↓ (day 3) U87MG and BT474C	-

sc: subcutaneous; NA: not available; →: no change in ^{18}F-FDG uptake; ↓↓: decrease in ^{18}F-FDG uptake compared with baseline; ↓: decreases in ^{18}F-FDG uptake compared with a control group; ↑↑: increases in ^{18}F-FDG uptake compared with baseline; ↑: increases in ^{18}F-FDG uptake compared with a control group. If both treatment sensitive and treatment resistant tumor models were analyzed, only the ^{18}F-FDG results from the tumor sensitive cell lines were included in the result column.

Table 4. ^{18}F-FLT PET of PI3K/AKT/mTOR inhibitor therapy

Target	Drug	Reference	Tumor placement	Cell line and origin	Treatments	Scan time (days after treatment initiation	Results	Same paper comparison with ^{18}F-FDG
mTOR	everolimus	[61]	sc	SKOV3 human ovarian adenocarcinoma	daily	2 and 7	↓↓	-
	everolimus	[59]	sc	SUDHL-1 and Karpas299 human lymphoma	daily/14 days	2 (Karpas299) and 5 (SUDHL)	↓↓	+
	everolimus	[66]	sc	H596 human lung carcinoma and HCT116 human colorectal carcinoma	daily	2/3 and 7/10	↓↓ (H596) → (HCT116)	+
	everolimus	[68]	sc	H727 human carcinoid cancer	daily	1, 3 and 10	↓ (day 10)	+
	rapamycin	[65]	sc	U87MG and LN-299 human glioblastoma	one dose	2	↓↓	+
	temsirolimus	[63]	sc	Daudi human B-lymphoblast	NA	2, 4, 7, 9 and 14	↓↓	+
	temsirolimus	[64]	sc	Granta-519 human mantle cell lymphoma	NA	1, 2, 4, 7, 9, 11 and 14	↓↓	+
	AZD8055	[58]	sc	U87MG human malignant glioma	daily	4	↓	+
PI3K/mTOR	BEZ235	[70]	sc	N87, MKN28 and MKN45 human gastric cancer	daily	2	↓	-
PI3-kinase	pictilisib (GDC-0941)	[71]	sc and orthotopic	HCT116 human colorectal carcinoma and U87 human glioma	twice daily/8 days	18 and 186 hours	↓↓ (18 h)	-

sc: subcutaneous; NA: not available; →: no change in ^{18}F-FLT uptake; ↓↓: decrease in ^{18}F-FLT uptake compared with baseline; ↓: decreases in ^{18}F-FLT uptake compared with a control group; ↑↑: increases in ^{18}F-FLT uptake compared with baseline; ↑: increases in ^{18}F-FLT uptake compared with a control group. If both treatment sensitive and treatment resistant tumor models were analyzed, only the ^{18}F-FLT results from the tumor sensitive cell lines were included in the result column.

Table 5. ^{18}F-FDG PET of angiogenic/vascular inhibitor therapy

Target	Drug	Reference	Tumor placement	Cell line and origin	Treatments	Scan time (days after treatment initiation)	Results	Same paper comparison with ^{18}F-FLT
VEGF-A	bevacizumab	[78]	orthotopic	U87 and U251 human glioblastoma	0, 3, 7 and 10	6	↓	+
	bevacizumab	[77]	orthotopic	MAS98.12 human breast carcinoma	one dose	1 and 3	↓↓ (day 1)	-
	bevacizumab	[76]	sc	A673 human rhabdomyosarcoma	one dose	2	↓↓	-
	PRS-050-PEG40	[76]	sc	A673 human rhabdomyosarcoma	one dose	2	↓↓	-
RAF/VEGFR2	AAL881	[66]	orthotopic	BN472 rat mammary tumors	daily	2 and 7	→	-
Tubulin	ombrabulin (AVE8062)	[79]	ip	HeyA8 human ovarian cancer	one dose	2 and 24 h	↓↓	-
VEGFR/PDGFR	sunitinib	[80]	orthotopic	U87MG human glioblastoma	5 dose/week for 2 weeks	3, 7, 10, 14 and 16	↓ (day 16)	+
Mulitkinase: RAF, VEGFR, PDGF, c-KIT, RET	sorafenib	[82]	sc	A673 human sarcoma	daily	1 and 6	↓↓ (day 6)	+
VEGFR1-3	axitinib	[84]	sc	U87MG human glioblastoma and MDA-MB-231 human breast cancer	daily/10 days	1, 3, 7 and 10	↓ (day 10)	+
VEGFR-2	ZD4190	[85]	sc	MDA-MB-435 human breast cancer	daily/3 days	1, 3 and 7	→	+

sc: subcutaneous; ip: intra peritoneal; →: no change in ^{18}F-FDG uptake; ↓↓: decrease in ^{18}F-FDG uptake compared with baseline; ↓: decreases in ^{18}F-FDG uptake compared with a control group; ↑↑: increases in ^{18}F-FDG uptake compared with baseline; ↑: increases in ^{18}F-FDG uptake compared with a control group. If both treatment sensitive and treatment resistant tumor models were analyzed, only the ^{18}F-FDG results from the tumor sensitive cell lines were included in the result column.

Table 6. ^{18}F-FLT PET of angiogenic/vascular inhibitor therapy

Target	Drug	Reference	Tumor placement	Cell line and origin	Treatments	Scan time (days after treatment initiation	Results	Same paper comparison with ^{18}F-FDG
VEGF-A	bevacizumab	[78]	orthotopic	U87MG and U251MG human glioblastoma	0, 3, 7 and 10	6	→	+
VEGFR/PDGFR	sunitinib	[80]	orthotopic	U87MG human glioblastoma	5/2 schedule	3, 7, 10, 14 and 16	↓ (from day 7)	+
	sunitinib	[81]	sc	U87MG human glioblastoma	daily/7 days	1, 3, 7 and 13	↓↓ (day 3 and 7)	-
Mulitkinase: RAF, VEGFR, PDGF, c-KIT, RET	sorafenib	[82]	sc	A673 human sarcoma	daily	1 and 5	↓↓	+
	sorafenib	[83]	im	FSall mouse fibrosarcoma	day 0 and 1	2 and 3	↓↓	-
VEGFR1-3	axitinib	[84]	sc	U87MG human glioblastoma and MDA-MB-231 human breast cancer	daily/10 days	1, 3, 7 and 10	↓ (day 3) U87-MG ↓↓ (day 7) MDA-MB-231	+
VEGFR-2	ZD4190	[85]	sc	MDA-MB-435 human breast cancer	daily/3 days	1, 3 and 7	↓↓ (day 1 and 3)	+

sc: subcutaneous; im: intra muscular; →: no change in ^{18}F-FLT uptake; ↓↓: decrease in ^{18}F-FLT uptake compared with baseline; ↓: decreases in ^{18}F-FLT uptake compared with a control group; ↑↑: increases in ^{18}F-FLT uptake compared with baseline; ↑: increases in ^{18}F-FLT uptake compared with a control group. If both treatment sensitive and treatment resistant tumor models were analyzed, only the ^{18}F-FLT results from the tumor sensitive cell lines were included in the result column.

Table 7. ^{18}F-FDG PET of other targeted therapies

Target	Drug	Reference	Tumor placement	Cell line and origin	Treatments	Scan time (days after treatment initiation)	Results	Same paper comparison with ^{18}F-FLT
MAPK pathway								
MEK1/2	PD0325901	[42]	sc	SKMEL-28 human melanoma, BT-474 human breast cancer	5 days weekly/3 weeks	week 1, 2, and 3	↓	+
MEK/Raf	RO5126766	[43]	sc	HCT116, COLO205, COLO320DM human colon cacinoma	daily	1, 2 and 3	↓↓	-
BRAF	PLX4720	[87]	sc	Lim2405 and HT29 human colorectal carcinoma	daily	3	→	+
Metabolism								
NAMPRT	daporinad (APO866)	[89]	sc	A2780 human ovarian carcinoma	twice daily	1, 2 and 7	↓↓ (day 7)	+
AMPK	metformin	[88]	sc	HT29 human colorectal carcinoma	one dose	1	↑↑	+
Amino acid metabolism	Top216	[90]	sc	A2780 human ovarian carcinoma	day 0 and 2	6 hours and day 1 and 6	↓↓	+
Aurora kinases								
Aurora B kinase	barasertib (AZD1152)	[93]	sc	HCT116 and SW620 human colorectal carcinoma	2 consecutive days/week/3 weeks	7, 14, 21, 26, 36, 43	→	+
Aurora B kinase	TAK-901	[94]	sc	HCT116 human colorectal carcinoma	twice daily for 2 days/week/2 weeks	4, 8, 11 and 15	→	+
HSP90	luminespib (AUY922)	[59]	sc	SUDHL-1 human lymphoma	daily	5	→	+
	tanespimycin (17AAG)	[96]	sc	BT474 human breast carcinoma	3 doses/one day	1, 8, 15, 22	→	-
Topoisomerase I	irinotecan	[97]	sc	HCT116 human colorectal carcinoma	weekly/3 weeks	1, 5, 8, and 15	↑ (day 8 and 15)	+
HDAC	belinostat	[100]	sc	A2780 human ovarian carcinoma	day 0-4 and 6-10	3, 6, and 10	↓ (day 10)	+
EMMPRIN	Anti-EMMPRIN	[113]	orthotopic	MIA PaCa-2 human pancreas carcinoma	day 0, 2, 7 and 10	7 and 14	↓↓ (day 14)	-
Proteasome	bortezomib	[118]	sc	CWR22 human prostate carcinoma	day 0, 2, 7, 10 and 14	1, 4, 8, 15 and 18	↓↓ (day 8)	-

sc: subcutaneous; →: no change in ^{18}F-FDG uptake; ↓↓: decrease in ^{18}F-FDG uptake compared with baseline; ↓: decreases in ^{18}F-FDG uptake compared with a control group; ↑↑: increases in ^{18}F-FDG uptake compared with baseline; ↑: increases in ^{18}F-FDG uptake compared with a control group. If both treatment sensitive and treatment resistant tumor models were analyzed, only the ^{18}F-FDG results from the tumor sensitive cell lines were included in the result column.

Table 8. ^{18}F-FLT PET of other targeted therapies

Target	Drug	Reference	Tumor placement	Cell line and origin	Treatments	Scan time (days after treatment initiation)	Results	Same paper comparison with ^{18}F-FDG
MAPK pathway								
MEK1/2	PD0325901	[42]	sc	SKMEL-28 human melanoma, BT-474 human breast cancer	5 days weekly/3 weeks	week 1, 2, and 3	↓↓	+
MEK1/2	PD0325901	[86]	sc	SKMEL-28 human melanoma and HCT116 human colorectal carcinoma	daily	1 and 10	↓	-
BRAF	PLX4720	[87]	sc	Lim2405 and HT29 human colorectal carcinoma	daily	4	↓↓	+
Metabolism								
NAMPRT	daporinad (APO866)	[89]	sc	A2780 human ovarian carcinoma	twice daily	1, 2 and 7	↓↓	+
AMPK	metformin	[88]	sc	HT29 human colorectal carcinoma	one dose	1	↓↓	+
Amino acid metabolism	arginine deiminase	[92]	sc	SKMEL-28 human melanoma	weekly/4 weeks	Once weekly prior to treatment	→	-
Amino acid metabolism	Top216	[119]	sc	A2780 human ovarian carcinoma	day 0 and 2	2 and 6 hours and day 1 and 6	↓↓	+
Amino acid metabolism	TP202377	[91]	sc	A2780 human ovarian carcinoma	one dose	6 hours, day 1 and 6	↓↓	-
Aurora kinases								
Aurora B kinase	barasertib (AZD1152)	[93]	sc	HCT116 and SW620 human colorectal carcinoma	2 consecutive days/week/3 weeks	8, 15, 22, 29, 37	↓ (8, 15, 22)	+
Aurora B kinase	TAK-901	[94]	sc	HCT116 human colorectal carcinoma	twice daily for 2 days/week/2 weeks	4, 9, 11 and 15	↓↓ (day 4 and 11)	+
Aurora A/B kinase	CCT129202	[95]	sc	HCT116 human colorectal carcinoma	daily	2 or 7	↓ (day 7)	-
HSP90	luminespib (AUY922)	[59]	sc	SUDHL-1 human lymphoma	daily	5	↓↓	+
Topoisomerase I								
Topoisomerase I	irinotecan	[97]	sc	HCT116 human colorectal carcinoma	weekly/3 weeks	1, 5, 8, and 15	↓↓ (1, 8, 15)	+
Topoisomerase I	irinotecan	[98]	sc	HCT116 human colorectal carcinoma	once weekly	8	↓↓	-
HDAC								
HDAC	belinostat	[100]	sc	A2780 human ovarian carcinoma	day 0-4 and 6-10	3, 6, and 10	→	+
HDAC	belinostat	[98]	sc	HCT116 human colorectal carcinoma	day 1-5 and 8-12	8	↓	-
HDAC	dacinostat (LAQ824)	[28]	sc	HCT116 human colorectal carcinoma	daily	2, 4 and 10	↓ (4 and 10)	-
HDAC	vorinostat (SAHA)	[99]	sc	HepG2 human hepatoma	5 days a week/3 weeks	8	↓↓	-
HDAC	ISAHA	[99]	sc	HepG2 human hepatoma	5 days a week/3 weeks	8	↓↓	-
FGFR	PD173074	[120]	sc	H-69 human SCLC	daily	7, 14	↓ (7 and 14)	-

sc: subcutaneous; SCLC: small cell lung cancer; →: no change in ^{18}F-FLT uptake; ↓↓: decrease in ^{18}F-FLT uptake compared with baseline; ↓: decreases in ^{18}F-FLT uptake compared with a control group; ↑↑: increases in ^{18}F-FLT uptake compared with baseline; ↑: increases in ^{18}F-FLT uptake compared with a control group. If both treatment sensitive and treatment resistant tumor models were analyzed, only the ^{18}F-FLT results from the tumor sensitive cell lines were included in the result column.

synthesis of thymidine ^{18}F-FLT uptake determined by PET will therefore not necessarily reflect the proliferative activity.

Response monitoring of targeted therapy

Many targeted therapies induce clinical responses; however, only in a subset of patients does the targeted therapy lead to tumor stasis or regression, increase in overall or progression free survival. The patients do not necessarily respond to the therapy even though the tumor expresses the target. Signaling pathways and cross-talks with other pathways can disturb identification of the 'correct' target and thereby how to predict the treatment outcome in an individual patient [37]. There is therefore clinical interest in understanding, which parameters are predictive for a positive treatment outcome and consequently if changes in ^{18}F-FLT and/or ^{18}F-FDG uptake measured by PET after initiation of a cancer treatment will be predictive for patient outcome.

Tyrosine kinase inhibitors

Various pre-clinical studies have analyzed ^{18}F-FDG and/or ^{18}F-FLT PET uptake following inhibition of different classes of tyrosine kinases (**Tables 1**, **2**). Both treatment with small molecule inhibitors and monoclonal antibodies have been studied. Compounds inhibiting members of the human epidermal growth factor receptor (HER/ErbB) have gained most interest where especially studies with drugs targeting the human epidermal growth factor receptor 1 (EGFR) have been conducted.

EGFR

Decrease in ^{18}F-FLT uptake has been observed as early as day 2-3 after initiation of treatment with the small molecule EFGR inhibitor erlotinib (**Table 2**) [38-40]. Ullrich et al. compared ^{18}F-FLT uptake with ^{18}F-FDG uptake and ^{18}F-FDG uptake was observed to be unchanged following treatment with erlotinib [38]. The suggestion was that ^{18}F-FDG more indirectly reflected tumor cell proliferation and therefore a therapy induced reduction in ^{18}F-FDG uptake was likely to be a later event; however, analysis of time points beyond day 4 was not covered in the study. In contrast to this, other studies found decreases in ^{18}F-FDG uptake 1 or 2 days after treatment initiation with the small molecule EFGR inhibitors erlotinib and gefitinib, respectively [37, 41]. Targeting of the mitogen-activated protein kinase (MAPK) signaling pathway by mitogen-activated protein kinase kinase (MEK)/Raf inhibitors, downstream of EGFR, also showed decrease in ^{18}F-FDG uptake [42, 43] (**Table 7**). Decrease in ^{18}F-FDG uptake after EGFR inhibition has been associated with translocation of GLUTs from the plasma membrane to the cytosol in some studies [37, 43] whereas another study observed unchanged GLUT-1 expression despite decreased ^{18}F-FDG uptake [41].

^{18}F-FLT uptake has been analyzed following treatment with the EGFR targeting monoclonal antibody cetuximab. ^{18}F-FLT uptake was found to decrease day 3 and day 6 after start of treatment with cetuximab in a human squamous cell carcinoma and human non-small cell lung cancer (NSCLC) tumor model, respectively [39, 44]. Another study observed no change in ^{18}F-FLT uptake despite treatment with cetuximab in a cetuximab-sensitive human colorectal carcinoma tumor model for a period of 7 days [45]. None of the studies compared ^{18}F-FLT uptake with ^{18}F-FDG.

HER2

Two studies analyzed uptake of ^{18}F-FDG after inhibition of the human epidermal growth factor receptor 2 (HER2) pathway (**Table 1**). Treatment with trastuzumab, a monoclonal antibody targeting HER2, did not change the uptake of ^{18}F-FDG during a three week treatment course in one study [46]. Contrary to this, another study found differences between a treatment and a control group after trastuzumab treatment, but not until 16 days after treatment initiation [47]. In a study by Shah et al. ^{18}F-FDG uptake was compared with ^{18}F-FLT uptake where ^{18}F-FLT uptake was decreased following one week of treatment with trastuzumab [46].

Pan-HER

Drugs targeting several members of the HER/ErbB family simultaneously have also been tested for their ability to change uptake of ^{18}F-FDG and ^{18}F-FLT early after treatment initiation (**Tables 1**, **2**). Both ^{18}F-FLT and ^{18}F-FDG uptake were decreased 3 and 6 days after start of daily treatments with canertinib (CI-

1033), a pan-HER inhibitor targeting all four members of the HER family [48]. Treatment with PKI-166 targeting both EGFR and HER2 resulted in decreases in ^{18}F-FDG uptake from day 7 and decreases in ^{18}F-FLT uptake from day 2 [30]. No change in ^{18}F-FDG uptake was observed after treatment with afatinib a selective inhibitor of EGFR, HER2 and HER4 and no comparison was made with ^{18}F-FLT [49].

c-KIT

Treatment with the c-KIT inhibitor imatinib resulted in dramatic and early decreases in ^{18}F-FDG uptake in tumor models displaying mutations in c-KIT, which is often observed in gastrointestinal stromal tumors (GIST) (**Table 1**) [50, 51]. Both number and activity of glucose transporters on the cell surface were decreased after imatinib treatment which were comparable with, and probably the cause of, the decrease in ^{18}F-FDG uptake [50]. Changes in ^{18}F-FDG uptake early after initiation of treatment with imatinib in GIST patients is a well-known predictor of patient outcome [52, 53].

c-MET

Inhibition of c-MET activation by the monoclonal antibody rilotumumab, as inhibits the binding of hepatocyte growth factor (HGF) to the c-MET receptor, induced decreases in both ^{18}F-FDG and ^{18}F-FLT uptake in the U87MG human glioblastoma model. ^{18}F-FDG and ^{18}F-FLT uptake were decreased day 2 and 4 after treatment start, respectively [54]. Furthermore, a dose-response relationship was evaluated with increasing doses of rilotumumab in U87MG tumor-bearing mice with ^{18}F-FDG PET [54]. Treatment effect was evaluated at baseline and day 7 after treatment with 10, 30, 100, 300 or 500 μg rilotumumab. Doses of 300 and 500 μg were similarly effective at reducing tumor growth and this was further reflected in a comparable inhibition of ^{18}F-FDG uptake [54]. In contrast to the early decrease in both ^{18}F-FDG and ^{18}F-FLT uptake after treatment with rilotumumab, inhibition of c-MET by the small molecule inhibitor crizotinib induced no change in ^{18}F-FDG uptake and ^{18}F-FLT uptake was not decreased until day 8 after treatment initiation with crizotinibin the U87MG tumor model [55]. Inhibition of c-MET with crizotinib in a GTL-16 human gastric cancer model caused ^{18}F-FLT decrease day 4 after treatment start whereas ^{18}F-FDG uptake was unchanged until day 13 [55]. Inhibition of c-MET with another small-molecule inhibitor, BAY 853474, induced reductions in both ^{18}F-FDG and ^{18}F-FLT uptake already from day 2 [56]. The monoclonal antibody against c-MET, CE-355621, inhibits ^{18}F-FDG accumulation in the U87MG human glioblastoma model [57]. Inhibition of ^{18}F-FDG accumulation following injection of CE-355621 was not compared with ^{18}F-FLT uptake.

In conclusion, the changes in ^{18}F-FDG and ^{18}F-FLT uptake after c-MET inhibition were most variable (**Tables 1**, **2**).

mTOR inhibitors

Activation of the phosphatidyl-inositol-3-kinase (PI3K)/AKT/mammalian target of rapamycin (mTOR) cascade signaling pathway regulates anti-proliferative and apoptotic functions and are involved in regulation of cell metabolism. Inhibition of mTOR and also other targets in this pathway will, at least theoretically, affect the cellular metabolism, expression of hexokinases and GLUT transporters and thereby the ^{18}F-FDG uptake in cancer cells [9, 41, 58]. Much interest has therefore been on analyzing ^{18}F-FDG uptake following inhibition of the PI3K/AKT/mTOR pathway and many pre-clinical studies have been conducted.

Everolimus, rapamycin and temsirolimus, small molecule inhibitors of mTOR, induced early reductions in both ^{18}F-FLT and ^{18}F-FDG from day 1 or 2 after initiation of treatment (**Tables 3**, **4**) [59-67].

Several studies have compared ^{18}F-FDG and ^{18}F-FLT uptake [59, 63-66]. Different mouse models of human cancer have been used, but despite the heterogeneous tumor models the early decreases in both ^{18}F-FDG and ^{18}F-FLT uptake were comparable. Most of the studies showed decreases in both ^{18}F-FLT and ^{18}F-FDG uptake after treatment initiation; however, in two studies ^{18}F-FDG was unchanged despite effective treatment of everolimus sensitive tumors [59, 68]. In one study ^{18}F-FDG and ^{18}F-FLT uptake on an individual tumor level day 1 and day 3 after treatment initiation predicted tumor growth despite no difference between the control and treatment group was observed [68]. Honer et al. analyzed the effect on ^{18}F-FLT and ^{18}F-FDG uptake in tumors arising from dif-

ferent cell lines characterized in advance as either sensitive or insensitive to everolimus treatment from *in vitro* assays [66]. When grown as tumor xenografts in nude mice both the growth of sensitive and insensitive tumors was inhibited with everolimus treatment. The growth inhibition of the insensitive tumors was suggested to be due to anti-angiogenic/vascular effects of everolimus, which was not evident *in vitro*. Interestingly, in the insensitive tumor models, in which everolimus had an effect on tumor growth, no change in either ^{18}F-FDG or ^{18}F-FLT uptake was observed and that led the authors to conclude that ^{18}F-FLT and ^{18}F-FDG PET may result in false-negative prediction of the possible anti-angiogenic/vascular effect of everolimus [66]. Inhibition of the mTOR kinase with AZD8055 resulted in decreases in both ^{18}F-FLT and ^{18}F-FDG uptake day 4 after treatment initiation. As early as one hour after injection with AZD8055 the ^{18}F-FDG uptake was reduced [58].

Inhibition of the PI3K/AKT/mTOR pathway by the AKT inhibitor AZD5363 resulted in decreases in ^{18}F-FDG uptake in two AZD5363-sensitive but not a AZD5363-resistant mouse tumor model 3 days after treatment initiation. Additionally, already 4 hours after one dose the ^{18}F-FDG uptake was decreased in a sensitive tumor model [69].

The dual PI3K/mTOR inhibitor BEZ235 significantly reduced ^{18}F-FLT uptake in a treatment-sensitive N87 human gastric cancer xenograft model whereas no change in ^{18}F-FLT uptake was observed in treatment-resistant tumor models [70]. Furthermore, Cawthorne et al. observed decreases in ^{18}F-FLT uptake already 16 hours after initiation of therapy with the PI3K inhibitor pictilisib (GDC-0941) in two pictilisib-sensitive tumor models but not a pictilisib-resistant tumor model [71].

Cejka et al. used ^{18}F-FDG PET to determine the optimal treatment dose of the mTOR inhibitor everolimus. Doses from 0.05 to 15 mg/kg were administered to mice bearing N87 gastric cancer xenografts and ^{18}F-FDG PET revealed that doses above 5 mg/kg did not reduce ^{18}F-FDG uptake further [67]. This was reflected in the anti-tumor activity of everolimus that reached a plateau with doses from 5 mg/kg and above.

Haagensen et al. investigated whether ^{18}F-FLT could be used to analyze the enhanced activity of a combination of a PI3K and a MEK inhibitor. They observed that treatment with the PI3K inhibitor pictilisib or the MEK inhibitor PD0325901 alone did not induce changes in ^{18}F-FLT uptake day 2 post injection whereas the combination treatment decreased the ^{18}F-FLT uptake [72].

Anti-angiogenic/vascular therapy

Treatment with anti-angiogenic compounds does only have an effect in a limited amount of a patients and identification of the subgroup of patients who is benefitting from anti-angiogenic therapy is difficult [73, 74]. Accordingly, several pre-clinical studies have investigated if either ^{18}F-FDG or ^{18}F-FLT PET could be of value in assessing whether or not a patient is responding to anti-angiogenic therapy. One of the treatment effects of anti-angiogenic therapy is normalization of the tumor vasculature [75]. Theoretically, it is therefore difficult to predict the outcome of both ^{18}F-FDG and ^{18}F-FLT uptake early after initiation of an anti-angiogenic therapy because normalization of tumor vasculature could cause a transient increase in cell proliferation and glucose consumption resulting from an enhancement of oxygen and nutrient supply to the cancer cells [75].

Following inhibition of tumor angiogenesis by the vascular endothelial growth factor A (VEGF-A) targeting antibody bevacizumab, ^{18}F-FDG uptake was decreased (**Table 5**) [76-78]. By dynamic ^{18}F-FDG PET analyses, treatment with bevacizumab was shown to reduce both the tumor perfusion and metabolism 24 hours post-treatment [77]. Targeting of VEGF-A by the PEGylated Anticalin Angiocal PRS-050-PEG40 did also reduce uptake of ^{18}F-FDG [76]. No influence on ^{18}F-FLT uptake was observed following inhibition of VEGF-A with bevacizumab [78].

Honer et al. found no change in ^{18}F-FDG uptake after treatment with AAL881, a dual RAF/VEGFR2 inhibitor [66]. As described in the previous section, anti-angiogenic/vascular effects of everolimus did not result in ^{18}F-FDG changes [66]. Targeting of the vasculature with the tubulin-binding agent ombrabulin (AVE8062) did very early after treatment initiation (2 and 24 hours) induce decrease in ^{18}F-FDG uptake [79].

Treatment with the compounds sunitinib [80, 81], sorafenib [82, 83], axitinib [84] and

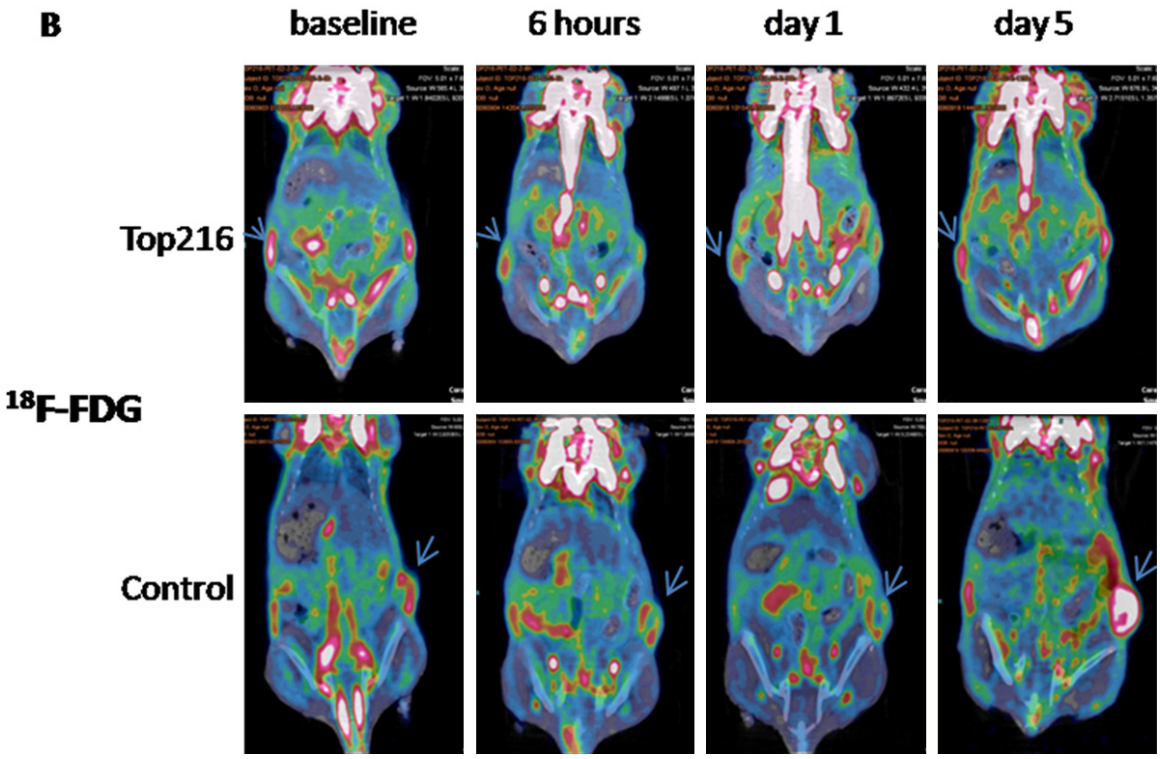

Figure 2. Examples of ^{18}F-FDG PET/CT images. Representative ^{18}F-FDG PET/CT images of a treatment mouse (top panel) and a control mouse (lower panel) scanned with ^{18}F-FDG at baseline and 6 hours, day 1 and day 5 after injections with one dose of Top216 or vehicle. Both mice carry the A2780 human ovarian carcinoma xenograft. The arrows point towards the tumors. The image is reproduced from [90].

ZD4190 [85], all targeting one or several of the VEGF receptors, induced decreases in ^{18}F-FLT uptake (**Table 6**). Sunitinib, sorafenib and axitinib did also decrease ^{18}F-FDG uptake; however, the reductions in ^{18}F-FDG uptake was a later event compared with the ^{18}F-FLT uptake (**Table 5**). Treatment with the VEGFR-2 targeting compound ZD4190 did not change the tumor ^{18}F-FDG uptake [85].

MAPK cascade

A few studies have analyzed how inhibitors of the MAPK signaling pathway influence the ^{18}F-FDG and ^{18}F-FLT uptake. Inhibition of MEK induced decreases in both ^{18}F-FDG and ^{18}F-FLT uptake (**Tables 7**, **8**) [42, 43, 86]. Inhibition of BRAF with the small molecule inhibitor PLX4720 induced decreases in ^{18}F-FLT uptake day 4 after treatment initiation in a mouse model of human colorectal cancer whereas no change in ^{18}F-FDG uptake was observed at day 3 after therapy initiation [87].

Metabolism

The anti-diabetes drug metformin, which modulate the cellular metabolism through AMP-activated protein kinase (AMPK) activation, is currently in several clinical trials in combination with different chemotherapeutic. Treatment of a mouse model of human colorectal carcinoma with metformin had a divergent effect on the uptake of ^{18}F-FDG and ^{18}F-FLT. ^{18}F-FDG uptake was found to be increased day 1 after initiation of therapy whereas the ^{18}F-FLT uptake was decreased [88]. The increase in ^{18}F-FDG uptake observed after treatment with metformin is probably because of externalization of GLUT transporters due to AMPK activation. Thus the positive effect of metformin on tumor growth would be overlooked if decreases in ^{18}F-FDG uptake are used as a surrogate marker of effective treatment. Difficulties with interpretation of ^{18}F-FDG uptake after initiation of cancer treatment could also arise in situations where glucose modulators are used either incidentally to treat other illness or as part of a combination treatment regime [88]. Treatment with another modulator of the cellular metabolism, the nicotinamide phosphoribosyltransferase (NAMPT) inhibitor daporinad (APO866) also decreased the ^{18}F-FLT uptake. Following treatment with daporinad ^{18}F-FDG

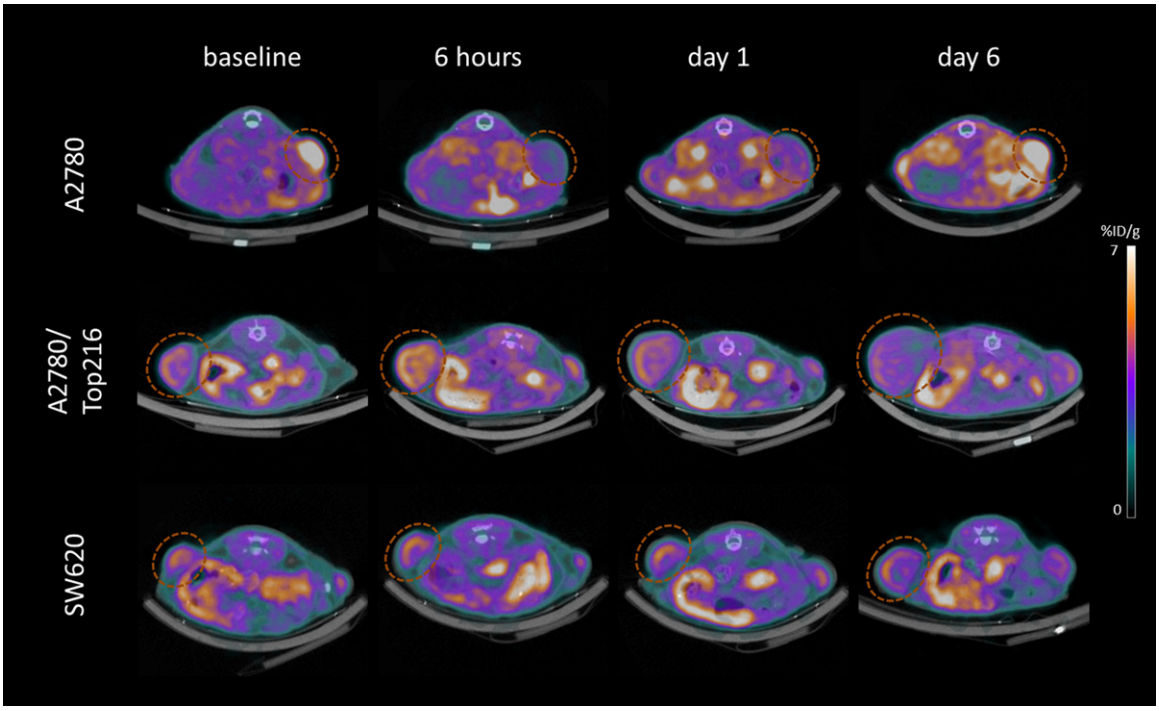

Figure 3. ^{18}F-FLT PET/CT images of treatment-sensitive and treatment-resistant tumors. Representative ^{18}F-FLT PET/CT images of a TP202377-sensitive tumor xenograft (A2780, upper panel) and two TP202377-resistant tumor xenografts (A2780/Top216 and SW620, middle and lower panel). ^{18}F-FLT uptake is measured by PET in the same mice at baseline and 6 hours, day 1 and day 6 after one injection with TP202377. The dotted circles delineate the tumors. The image is reproduced from [91].

uptake was also decreased, but later compared to ^{18}F-FLT uptake [89].

Targeting amino acid metabolism with Top216/TP202377 decreased both ^{18}F-FDG and ^{18}F-FLT uptake (**Figure 2**) [90, 91], whereas treatment with the arginine deiminase did not induce a response in the ^{18}F-FLT uptake [92]. Treatment with both Top216 and TP202377 induced decrease in ^{18}F-FLT uptake as early as 2 and 6 hours post injection where it was possible to separate responding from non-responding tumors (**Figure 3**) [90, 91].

Aurora kinases

Inhibition of mitosis through targeting of the aurora kinases, a family of serine kinases that play a role in the regulation of mitosis, has been investigated with both ^{18}F-FDG and ^{18}F-FLT PET. Treatment with the Aurora B kinase inhibitors barasertib (AZD1152) and TAK-901 induced reductions in ^{18}F-FLT uptake (**Table 8**) [93, 94]. For comparison, no change was observed in ^{18}F-FDG uptake following treatment initiation with either barasertib or TAK-901 (**Table 7**). Likewise, did the dual Aurora A/B kinase inhibitor CCT129202 induce decreases in ^{18}F-FLT uptake but no comparison was made with ^{18}F-FDG [95].

HSP90

The heat shock protein 90 (HSP90) inhibitor luminespib (AUY922) inhibited uptake of ^{18}F-FLT in a SUDHL-1 lymphoma model whereas no change was observed for ^{18}F-FDG uptake [59]. Furthermore, did the HSP90 inhibitor tanespimycin (17AAG) not change ^{18}F-FDG uptake in a BT474 breast cancer model after initiation of effective treatment [96].

Topoisomerase I

Inhibition of topoisomerase I by irinotecan decreased the ^{18}F-FLT uptake already from day 1 after initiation of treatment (**Table 8**) [97, 98]. This was in contrast to the ^{18}F-FDG uptake which were shown to be increased from day 8 following treatment initiation with irinotecan [97]. Inhibition of DNA replication by targeting topoisomerase I with irinotecan

Table 9. ^{18}F-FDG PET of chemotherapeutics

Target	Drug	Reference	Tumor placement	Cell line and origin	Treatments	Scan time (days after treatment initiation)	Results	Same paper comparison with ^{18}F-FLT
Microtubule	docetaxel	[101]	sc	22Rv1 human prostate carcinoma	weekly/2 weeks	2 weeks	→	+
	albumine-bound paclitaxel	[102]	orthotopic	MDA-MB-435 human melanoma	every other day/3 doses total	3, 7, 14 and 21	↑ (day 7)	-
	patupilone	[66]	orthotopic	BN472 rat mammary tumors	one dose	2 and 6	↓↓	-
Alkylating agents	cyclophosphamide	[64]	sc	Granta-519 human mantle cell lymphoma	one dose	1, 2, 4, 7, 9, 11 and 14	↓↓ (day 2 and 11)	+
	cyclophosphamide	[63]	sc	Daudi human B-lymphoblast	one dose	2, 4, 7, 9 and 24	↓↓	-
	cyclophosphamide	[62]	sc	Daudi human B-lymphoblast	NA	2, 4, 7, 9 and 14	↓↓ (day 2 and 4)	+
	temozolomide	[78]	orthotopic	U87 and U251 human glioblastoma	day 0, 3, 7 and 10	6	↓	+
Platinum analogues	cisplatin	[107]	sc	NCCIT human testicular embryonal carcinoma	one dose	2, 4 and 7	↓↓ (day 7)	-
	cisplatin	[108]	sc	PEO1 and PEO4 human ovarian adenocarcinoma	3 consecutive days	4	↓↓	+
	cisplatin	[27]	sc	RIF-1 murine fibrosarcoma	one dose	1 and 2	↓	+
Antimetabolites	5-fluorouracil	[24]	sc	RIF-1 murine fibrosarcoma	one dose	1 and 2	↓ (day 2)	+
	methotrexate	[112]	sc	MC4-L2 and MC7-L1 murine mammary ductal carcinoma	one dose	1, 7 and 14	→	-
	gemcitabine	[113]	orthotopic	MIA PaCa-2 human pancreas carcinoma	day 0 and 7	7 and 14	↓↓ (day 7 and 14)	-
Anthracyclines	doxorubicin	[117]	sc	SUDHL-4 human large B-cell lymphoma	one dose	2	↑↑	+
	doxorubicin	[112]	sc	MC4-L2 and MC7-L1 murine mammary ductal carcinoma	one dose	1, 7 and 14	↓↓	-
	liposomal doxorubicin	[115]	sc	UM-SCC-22B human head and neck squamous cell carcinoma	day 0 and 2	2 and 4	↓↓ (day 4)	+
	liposomal doxorubicin	[114]	sc	C26 murine colorectal carcinoma	one dose	1	→	+

sc: subcutaneous; NA: not available; →: no change in ^{18}F-FDG uptake; ↓↓: decrease in ^{18}F-FDG uptake compared with baseline; ↓: decreases in ^{18}F-FDG uptake compared with a control group; ↑↑: increases in ^{18}F-FDG uptake compared with baseline; ↑: increases in ^{18}F-FDG uptake compared with a control group. If both treatment sensitive and treatment resistant tumor models were analyzed, only the ^{18}F-FDG results from the tumor sensitive cell lines were included in the result column.

Table 10. ^{18}F-FLT PET of chemotherapeutics

Target	Drug	Reference	Tumor placement	Cell line and origin	Treatments	Scan time (days after treatment initiation	Results	Same paper comparison with ^{18}F-FDG
Microtubule	docetaxel	[101]	sc	22Rv1 human prostate carcinoma	weekly/2 weeks	2 weeks	↓↓	+
	JAC106	[103]	sc	SW620 human colorectal adeno-carcinoma and KB-V1 human cervix carcinoma	day 0 and 7	3 and 7/8	↓↓ (day 3)	-
	patupilone	[104]	sc	RIF-1 mouse fibrosarcoma	one dose	1, 2, 3 and 6	↓	-
Alkylating agents	cyclophosphamide	[64]	sc	Granta-519 human mantle cell lymphoma	one dose	1, 2, 4, 7, 9, 11 and 14	↓↓ (day 2, 4, 7, 9, 11 and 14)	+
	cyclophosphamide	[62]	sc	Daudi human B-lymphoblast	NA	2, 4, 7, 9 and 14	↓↓ (day 7, 9 and 14)	+
	temozolomide	[78]	orthotopic	U87 and U251 human glioblastoma	day 0, 3, 7 and 10	6	↓	+
	temozolomide	[106]	sc and orthotopic	Gli36dEGFR-1 and Gli36dEGFR-2 human glioblastoma	daily/7 days	2	↓	-
Platinum analogues	cisplatin	[108]	sc	PEO1 and PEO4 human ovarian adenocarcinoma	3 consecutive days	4	↓↓	+
	cisplatin	[27]	sc	RIF-1 mouse fibrosarcoma	one dose	1 and 2	↓	+
Antimetabolites	5-fluorouracil	[24]	sc	RIF-1 mouse fibrosarcoma	one dose	1 and 2	↓	+
	5-fluorouracil	[109]	sc	RIF-1 mouse fibrosarcoma	one dose	1 hour	↑	-
	5-fluorouracil	[111]	sc	HT29 human colorectal carcinoma	one dose	1	↑↑	-
	5-fluorouracil	[110]	sc	HT29 human colorectal carcinoma	one dose	1	↑	-
Anthracyclines	doxorubicin	[117]	sc	SUDHL-4 human large B-cell lymphoma	one dose	2	↓↓	+
	doxorubicin	[116]	sc	SUDHL-4 human large B-cell lymphoma	one dose	1, 5 and 9	↓↓ (day 1 and 5)	-
	liposomal doxorubicin	[115]	sc	UM-SCC-22B human head and neck squamous cell carcinoma	day 0 and 2	2 and 4	↓↓ (day 4)	+
	liposomal doxorubicin	[114]	sc	C26 murine colorectal carcinoma	one dose	1	↓↓	+

sc: subcutaneous; NA: not available; →: no change in ^{18}F-FLT uptake; ↓↓: decrease in ^{18}F-FLT uptake compared with baseline; ↓: decreases in ^{18}F-FLT uptake compared with a control group; ↑↑: increases in ^{18}F-FLT uptake compared with baseline; ↑: increases in ^{18}F-FLT uptake compared with a control group. If both treatment sensitive and treatment resistant tumor models were analyzed, only the ^{18}F-FLT results from the tumor sensitive cell lines were included in the result column.

did accordingly have the opposite effect on the ^{18}F-FLT and ^{18}F-FDG uptake.

Histone deacetylase

After treatment initiation with the histone deacetylase (HDAC) inhibitors belinostat, dacinostat (LAQ824) and vorinostat (SAHA)/ISAHA the uptake of ^{18}F-FLT was shown to be decreased in all but one case (**Table 8**) [28, 98, 99]. In one study, the ^{18}F-FLT uptake was compared with ^{18}F-FDG after initiation of treatment with belinostat and it was observed that the ^{18}F-FDG uptake was decreased whereas no change in ^{18}F-FLT uptake was found after treatment with the compound for a period of 10 days [100].

Response monitoring of chemotherapeutics

Several studies have analyzed ^{18}F-FDG and ^{18}F-FLT uptake with PET in pre-clinical tumor models after treatment with compounds from different classes of chemotherapeutics. Many chemotherapeutics directly induces cell-cycle arrest and therefore uptake of the cell proliferation tracer ^{18}F-FLT has been widely studied.

Microtubule targeting agents

The influence on ^{18}F-FDG uptake following treatment with compounds disturbing the microtubules has shown to be quite variable. Following treatment with docetaxel, the ^{18}F-FDG uptake was found to be unchanged despite effective treatment [101]. Treatment with nanoparticle albumin-bound paclitaxel induced increases in ^{18}F-FDG uptake day 7 which were associated with an inflammatory reaction in the tumor tissue [102]. Oppositely, treatment with one dose of the microtubule stabilizer patupilone induced reductions in ^{18}F-FDG uptake day 2 and 6 post injection (**Table 9**) [66].

Treatment with chemotherapeutic compounds targeting the microtubules induced a more consistent response in the ^{18}F-FLT uptake when compared with the ^{18}F-FDG uptake. Treatment with docetaxel, JAC106 and patupilone all induced decreases in ^{18}F-FLT uptake although there was variation in relation to at what time after first injection the decrease was observed (**Table 10**) [101, 103, 104]. Ebenhan et al. observed decreases in ^{18}F-FLT uptake already from day 1 after one dose of patupilone, reductions were observed after 3 days of JAC106 treatment [103] and not until 2 weeks after treatment initiation with docetaxel was reductions in ^{18}F-FLT uptake observed [101].

Treatment with paclitaxel in combination with carboplatin decreased uptake of both ^{18}F-FDG and ^{18}F-FLT in a mouse model of human ovarian cancer [105].

DNA damaging agents

Analysis of both ^{18}F-FDG and ^{18}F-FLT uptake by PET has been investigated following initiation of treatment with different DNA damaging compounds. Both alkylating agents and platinum analogues induce DNA damage resulting in cell cycle arrest and apoptosis and have therefore attracted interest with regard to response monitoring with both ^{18}F-FDG and ^{18}F-FLT PET.

Alkylating agents

Several studies have analyzed how different alkylating agents affect the uptake of ^{18}F-FDG and ^{18}F-FLT in pre-clinical models of human cancer. Treatment with cyclophosphamide induced decreases in ^{18}F-FDG uptake already day 2 after treatment initiation in different tumor models (**Table 9**) [62-64]. ^{18}F-FLT uptake was also shown to decrease early following treatment with cyclophosphamide, however in one study it was not observed until the 7th day after treatment initiation (**Table 10**) [62, 64].

Treatment with temozolomide caused reductions in both ^{18}F-FDG and ^{18}F-FLT uptake day 6 after treatment initiation in an orthotopic model of human glioblastoma [78]. In another study, 2 days after temozolomide therapy initiation, ^{18}F-FLT uptake was decreased in both a subcutaneous and an intra-cranially implanted glioblastoma model [106]. Furthermore, a positive correlation was observed between changes in ^{18}F-FLT accumulation day 2 and changes in tumor size later on.

Platinum analogues

Treatment with the platinum analogue cisplatin reduced both ^{18}F-FDG and ^{18}F-FLT uptake early after initiation of treatment in several independent studies (**Tables 9**, **10**) [27, 107, 108].

Antimetabolites

The use of ^{18}F-FLT PET for measurement of treatment effect with the pyrimidine analogue 5-fluorouracil (5-FU) has attracted a special attention because 5-FU directly affects the thymidylate synthase (TS), a key enzyme involved in the DNA synthesis. Inhibition of TS by 5-FU results in rapid decrease in the cellular thymidine phosphate pool and the cancer cells may respond to this shortage by increasing TK1 and nucleoside transporter activity. How ^{18}F-FLT uptake will be influenced by 5-FU treatment is difficult to predict, because the cancer treatment with 5-FU can result in a temporary increase in ^{18}F-FLT retention and different outcomes on the ^{18}F-FLT uptake has consequently been observed following treatment with 5-FU.

Studies on ^{18}F-FLT uptake in RIF-1 tumor bearing mice after injection with 5-FU have showed that one hour after injection of 5-FU, TS inhibition was imaged by an increase in the ^{18}F-FLT uptake probably being due to redistribution of nucleoside transporters to the cell membrane [109]. Day 1 and 2 after 5-FU treatment of the same RIF-1 tumor model the ^{18}F-FLT uptake was decreased compared with a vehicle treated control [24]. Response monitoring of 5-FU treatment with ^{18}F-FLT PET of a HT29 human colorectal adenocarcinoma model has been analyzed in two studies (**Table 10**). Both studies observed increase in ^{18}F-FLT uptake 24 hours after injection of 5-FU [110, 111]. Hong et al analyzed the kinetic parameters of the ^{18}F-FLT uptake by a two hours dynamic PET imaging 24 hours after injection with 5-FU and showed that the parameters related to ^{18}F-FLT retention was significantly higher in the treatment compared to the control group whereas the parameters related to dephosphorylation of ^{18}F-FLT monophosphate was conversely significantly lower in the treatment compared to the control group [110].

One study compared the ^{18}F-FLT uptake following 5-FU treatment with ^{18}F-FDG uptake and it was found that ^{18}F-FDG uptake was decreased 2 days after initiation of treatment (**Table 9**) compared to FLT uptake which was decreased on both day 1 and 2 following treatment initiation [24].

The antifolate compound methotrexate did not change the ^{18}F-FDG uptake until 14 days after treatment initiation [112] whereas the nucleoside analogue gemcitabine was shown to decrease uptake of ^{18}F-FDG day 7 and day 14 after initiation of treatment [113].

Anthracyclines

Treatment with the anthracyclines doxorubicin or liposomal doxorubicin (pegylated liposome-encapsulated doxorubicin) both induced decreases in ^{18}F-FLT within 1 to 4 days after initiation of treatment (**Table 10**) [114-117]. Interestingly, changes in ^{18}F-FDG uptake varied considerably after initiation of doxorubicin or liposomal doxorubicin treatment (**Table 9**). Two days after injection with one dose of doxorubicin one study observed that ^{18}F-FDG uptake in the treatment group was significantly increased compared with baseline uptake [117]. In contrast to this up-regulation another study observed significant decrease in ^{18}F-FDG uptake already day 1 after initiation of doxorubicin treatment [112]. The two studies used different tumor models which could be an explanation on the divergent outcome. Following injection with liposomal doxorubicin one study failed to detect an ^{18}F-FDG response already day 1 after liposomal doxorubicin injection, which is in line with another study in which FDG uptake was observed to be unchanged until day 4 after treatment initiation [114, 115].

Conclusions

A non-invasive method to measure early treatment effect of cancer therapeutics is requested in many settings both during development of new therapies but also during treatment with already approved therapies. A comprehensive amount of pre-clinical studies have investigated the use of ^{18}F-FDG and ^{18}F-FLT PET for treatment monitoring. ^{18}F-FDG and ^{18}F-FLT PET have in both pre-clinical and clinical studies been evaluated as imaging biomarkers that can predict and assess responses to various types of anti-cancer therapies this being different targeted therapies but also conventional chemotherapeutics. The results from the pre-clinical studies are variable, in some studies early changes in ^{18}F-FDG and ^{18}F-FLT uptake predict later tumor regression and in other studies no changes in tracer uptake are observed despite the treatment being effective. Overall both ^{18}F-FDG and/or ^{18}F-FLT uptake were decreased following treatment initiation with different inhibitors targeting the HER fam-

ily; however, some studies observed no change in tracer uptake despite effective treatment. Differences in ^{18}F-FDG and ^{18}F-FLT uptake following treatment with the same anti-cancer compound are probably due to variations in the experimental protocols or the use of different tumor models. Both ^{18}F-FDG and ^{18}F-FLT were reduced after treatment with inhibitors of the PI3K/AKT/mTOR pathway while after treatment with the chemotherapeutic 5-FU different responses in ^{18}F-FLT uptake was observed.

The mechanism behind changes in tracer uptake after treatment initiation seems to be very complex and dependent on both tumor type, mode of action of the anti-cancer drug and at what time after treatment initiation the tracer uptake is being studied.

Selection of patients into responders and non-responders based on non-invasive PET scans holds a large potential and our prediction is that ^{18}F-FDG PET and/or ^{18}F-FLT PET will increasingly be included in future (adaptive) study designs when new cancer treatments are being developed and tested. The use of PET imaging for biological characteristics during the early pre-clinical animal experiments can improve knowledge of drug candidates and maybe help selecting which imaging biomarkers could be included in subsequent clinical studies [8]. Furthermore we foresee that ^{18}F-FDG and ^{18}F-FLT PET will be applied to predict treatment effect in more cancer types and for more treatment regimens than today thereby help implementing the practice of precision medicine. However, the current data clearly underlines that in each specific case, pre-clinical testing of ^{18}F-FDG and ^{18}F-FLT should be performed to validate the value of the PET tracers.

Acknowledgements

The generous support of the research into the PET imaging in cancer in form of unrestriced grants from the Innovation Fund Denmark, the John and Birthe Meyer Foundation, the Danish Medical Research Council, the Rigshospitalets Research Foundation, the Svend Andersen Foundation, the AP Moller Foundation, the Novo Nordisk Foundation, the Lundbeck Foundation and the Danish Cancer Society is gratefully acknowledged. The authors declare no conflicts of interest.

Address correspondence to: Dr. Andreas Kjaer, Department of Clinical Physiology, Nuclear Medicine & PET (KF-4012), Rigshospitalet, National University Hospital, Blegdamsvej 9, DK-2100 Copenhagen, Denmark. E-mail: akjaer@sund.ku.dk

References

[1] Buyse M, Thirion P, Carlson RW, Burzykowski T, Molenberghs G, Piedbois P. Relation between tumour response to first-line chemotherapy and survival in advanced colorectal cancer: a meta-analysis. Meta-Analysis Group in Cancer. Lancet 2000; 356: 373-378.

[2] Douillard JY, Cunningham D, Roth AD, Navarro M, James RD, Karasek P, Jandik P, Iveson T, Carmichael J, Alakl M, Gruia G, Awad L, Rougier P. Irinotecan combined with fluorouracil compared with fluorouracil alone as first-line treatment for metastatic colorectal cancer: a multicentre randomised trial. Lancet 2000; 355: 1041-1047.

[3] Schiller JH, Harrington D, Belani CP, Langer C, Sandler A, Krook J, Zhu J, Johnson DH. Comparison of four chemotherapy regimens for advanced non-small-cell lung cancer. N Engl J Med 2002; 346: 92-98.

[4] Wahl RL, Jacene H, Kasamon Y, Lodge MA. From RECIST to PERCIST: Evolving Considerations for PET response criteria in solid tumors. J Nucl Med 2009; 50 Suppl 1: 122S-150S.

[5] Hess S, Blomberg BA, Zhu HJ, Høilund-Carlsen PF, Alavi A. The pivotal role of FDG-PET/CT in modern medicine. Acad Radiol 2014; 21: 232-249.

[6] Barwick T, Bencherif B, Mountz JM, Avril N. Molecular PET and PET/CT imaging of tumour cell proliferation using F-18 fluoro-L-thymidine: a comprehensive evaluation. NuclMed Commun 2009; 30: 908-917.

[7] Ben-Haim S, Ell P. 18F-FDG PET and PET/CT in the evaluation of cancer treatment response. J Nucl Med 2009; 50: 88-99.

[8] Soloviev D, Lewis D, Honess D, Aboagye E. [(18)F]FLT: an imaging biomarker of tumour proliferation for assessment of tumour response to treatment. Eur J Cancer 2012; 48: 416-424.

[9] Kelloff GJ, Hoffman JM, Johnson B, Scher HI, Siegel BA, Cheng EY, Cheson BD, O' shaughnessy J, Guyton KZ, Mankoff DA, Shankar L, Larson SM, Sigman CC, Schilsky RL, Sullivan DC. Progress and promise of FDG-PET imaging for cancer patient management and oncologic drug development. Clin Cancer Res 2005; 11: 2785-808.

[10] Chalkidou A, Landau DB, Odell EW, Cornelius VR, O'Doherty MJ, Marsden PK. Correlation be-

tween Ki-67 immunohistochemistry and 18F-fluorothymidine uptake in patients with cancer: A systematic review and meta-analysis. Eur J Cancer 2012; 48: 3499-513.
[11] Tehrani OS, Shields AF. PET Imaging of Proliferation with Pyrimidines. J Nucl Med 2013; 54: 903-912.
[12] Herrmann K, Buck AK. Proliferation Imaging with 18F-Fluorothymidine PET/Computed Tomography. PET Clin 2014; 9: 331-338.
[13] Paesmans M, Sculier JP, Libert P, Bureau G, Dabouis G, Thiriaux J, Michel J, van Cutsem, Sergysels R, Mommen P, Klastersky J. Response to chemotherapy has predictive value for further survival of patients with advanced non-small cell lung cancer: 10 years experience of the European Lung Cancer Working Party. Eur J Cancer 1997; 33: 2326-2332.
[14] Eisenhauer EA, Therasse P, Bogaerts J, Schwartz LH, Sargent D, Ford R, Dancey J, Arbuck S, Gwyther S, Mooney M, Rubinstein L, Shankar L, Dodd L, Kaplan R, Lacombe D, Verweij J. New response evaluation criteria in solid tumours: revised RECIST guideline (version 1.1). Eur J Cancer 2009; 45: 228-247.
[15] Bos R, van der Hoeven JJ, van der Wall, van der Groep, van Diest PJ, Comans EF, Joshi U, Semenza GL, Hoekstra OS, Lammertsma AA, Molthoff CF. Biologic correlates of (18)fluorodeoxyglucose uptake in human breast cancer measured by positron emission tomography. J Clin Oncol 2002; 20: 379-387.
[16] Som P, Atkins HL, Bandoypadhyay D, Fowler JS, MacGregor RR, Matsui K, Oster ZH, Sacker DF, Shiue CY, Turner H, Wan CN, Wolf AP, Zabinski SV. A fluorinated glucose analog, 2-fluoro-2-deoxy-D-glucose (F-18): nontoxic tracer for rapid tumor detection. J Nucl Med 1980; 21: 670-675.
[17] Hsu PP, Sabatini DM. Cancer cell metabolism: Warburg and beyond. Cell 2008; 134: 703-707.
[18] Shields AF, Grierson JR, Dohmen BM, Machulla HJ, Stayanoff JC, Lawhorn-Crews JM, Obradovich JE, Muzik O, Mangner TJ. Imaging proliferation in vivo with [F-18]FLT and positron emission tomography. Nat Med 1998; 4: 1334-1336.
[19] Kong XB, Zhu QY, Vidal PM, Watanabe KA, Polsky B, Armstrong D, Ostrander M, Muchmore E, Chou TC. Comparisons of anti-human immunodeficiency virus activities, cellular transport, and plasma and intracellular pharmacokinetics of 3'-fluoro-3'-deoxythymidine and 3"-azido-3-"deoxythymidine. Antimicrob Agents Chemother 1992; 36: 808-818.
[20] Been LB, Suurmeijer AJ, Cobben DC, Jager PL, Hoekstra HJ, Elsinga PH. [18F]FLT-PET in oncology: current status and opportunities. Eur J Nucl Med MolImaging 2004; 31: 1659-1672.
[21] Sherley JL, Kelly TJ. Regulation of human thymidine kinase during the cell cycle. J Biol Chem 1988; 263: 8350-8358.
[22] Arnér ESJ, Eriksson S. Mammalian deoxyribonucleoside kinases. Pharmacology & Therapeutics 1995; 67: 1-32.
[23] Rasey JS, Grierson JR, Wiens LW, Kolb PD, Schwartz JL. Validation of FLT uptake as a measure of thymidine kinase-1 activity in A549 carcinoma cells. J Nucl Med 2002; 43: 1210-1217.
[24] Barthel H, Cleij MC, Collingridge DR, Hutchinson OC, Osman S, He Q, Luthra SK, Brady F, Price PM, Aboagye EO. 3'-Deoxy-3'-[18F]Fluorothymidine as a New Marker for Monitoring Tumor Response to Antiproliferative Therapy in Vivo with Positron Emission Tomography. Cancer Res 2003; 63: 1-9.
[25] Buck AK, Halter G, Schirrmeister H, Kotzerke J, Wurziger I, Glatting G, Mattfeldt T, Neumaier B, Reske SN, Hetzel M. Imaging proliferation in lung tumors with PET: 18F-FLT versus 18F-FDG. J Nucl Med 2003; 44: 1426-1431.
[26] Francis DL, Freeman A, Visvikis D, Costa DC, Luthra SK, Novelli M, Taylor I, Ell PJ. In vivo imaging of cellular proliferation in colorectal cancer using positron emission tomography. Gut 2003; 52: 1602-1606.
[27] Leyton J, Latigo JR, Perumal M, Dhaliwal H, He Q, Aboagye EO, Leyton J. Early Detection of Tumor Response to Chemotherapy by 3"-Deoxy-3-"[18F]Fluorothymidine Positron Emission Tomography: The Effect of Cisplatin on a Fibrosarcoma Tumor Model In vivo. Cancer Res 2005; 65: 1-10.
[28] Leyton J, Leyton J, Alao JP, Da Costa M, Alao JP, Da Costa M, Stavropoulou AV, Stavropoulou AV, Latigo JR, Latigo JR, Perumal M, Pillai R, Pillai R, He Q, Atadja P, Lam EW, Atadja P, Lam EW, Workman P, Vigushin DM, Workman P, Vigushin DM, Aboagye EO. In vivo Biological Activity of the Histone Deacetylase Inhibitor LAQ824 Is detectable with 3"-Deoxy-3-"[18F]Fluorothymidine Positron Emission Tomography. Cancer Res 2006; 66: 1-10.
[29] Vesselle H, Grierson J, Muzi M, Pugsley JM, Schmidt RA, Rabinowitz P, Peterson LM, Vallieres E, Wood DE. In vivo validation of 3"deoxy-3-"[(18)F]fluorothymidine ([(18)F]FLT) as a proliferation imaging tracer in humans: correlation of [(18)F]FLT uptake by positron emission tomography with Ki-67 immunohistochemistry and flow cytometry in human lung tumors. Clin Cancer Res 2002; 8: 3315-3323.
[30] Waldherr C, Mellinghoff IK, Tran C, Halpern BS, Rozengurt N, Safaei A, Weber WA, Stout D,

Satyamurthy N, Barrio J, Phelps ME, Silverman DH, Sawyers CL, Czernin J. Monitoring antiproliferative responses to kinase inhibitor therapy in mice with 3“-deoxy-3-”18F-fluorothymidine PET. J Nucl Med 2005; 46: 1-7.

[31] Buck AK, Schirrmeister H, Hetzel M, Der von HM, Halter G, Glatting G, Mattfeldt T, Liewald F, Reske SN, Neumaier B. 3-deoxy-3-[(18)F]fluorothymidine-positron emission tomography for noninvasive assessment of proliferation in pulmonary nodules. Cancer Res 2002; 62: 3331-3334.

[32] Yamamoto Y, Nishiyama Y, Ishikawa S, Nakano J, Chang SS, Bandoh S, Kanaji N, Haba R, Kushida Y, Ohkawa M. Correlation of 18F-FLT and 18F-FDG uptake on PET with Ki-67 immunohistochemistry in non-small cell lung cancer. Eur J Nucl Med MolImaging 2007; 34: 1610-1616.

[33] Yap CS, Czernin J, Fishbein MC, Cameron RB, Schiepers C, Phelps ME, Weber WA. Evaluation of thoracic tumors with 18F-fluorothymidine and 18F-fluorodeoxyglucose-positron emission tomography. Chest 2006; 129: 393-401.

[34] Paproski RJ, Wuest M, Jans HS, Graham K, Gati WP, McQuarrie S, McEwan A, Mercer J, Young JD, Cass CE. Biodistribution and uptake of 3“-deoxy-3-”fluorothymidine in ENT1-knockout mice and in an ENT1-knockdown tumor model. J Nucl Med 2010; 51: 1447-1455.

[35] Paproski RJ, Ng AM, Yao SY, Graham K, Young JD, Cass CE. The role of human nucleoside transporters in uptake of 3“-deoxy-3-” fluorothymidine. Mol Pharmacol 2008; 74: 1372-1380.

[36] Zhang CC, Yan Z, Li W, Kuszpit K, Painter CL, Zhang Q, Lappin PB, Nichols T, Lira ME, Affolter T, Fahey NR, Cullinane C, Spilker M, Zasadny K, O’Brien P, Buckman D, Wong A, Christensen JG. [(18)F]FLT-PET imaging does not always “light up” proliferating tumor cells. Clin Cancer Res 2012; 18: 1303-1312.

[37] Su H, Bodenstein C, Dumont RA, Seimbille Y, Dubinett S, Phelps ME, Herschman H, Czernin J, Weber W. Monitoring tumor glucose utilization by positron emission tomography for the prediction of treatment response to epidermal growth factor receptor kinase inhibitors. Clin Cancer Res 2006; 12: 1-10.

[38] Ullrich RT, Zander T, Neumaier B, Koker M, Shimamura T, Waerzeggers Y, Borgman CL, Tawadros S, Li H, Sos ML, Backes H, Shapiro GI, Wolf J, Jacobs AH, Thomas RK, Winkeler A, Cologne GM, (CMMC) CG, Cologne GD, Oncology DO, Medicine DO, Fulda GK, Society DG. Early Detection of Erlotinib Treatment Response in NSCLC by 3’-Deoxy-3’ [18F]-Fluoro-L-Thymidine ([18F]FLT) Positron Emission Tomography (PET). You M, ed. PLoS One 2008; 3: 1-6.

[39] Atkinson D, Medicine PP, Clarke M, Clinic RM, Mladek A, Carlson B, Trump D, Jacobson M, Kemp B, Lowe V, Sarkaria J, Atkinson DM, Clarke MJ, Mladek AC, Carlson BL, Trump DP, Jacobson MS, Kemp BJ, Lowe VJ, Sarkaria JN. Using fluorodeoxythymidine to monitor anti‐ EGFR inhibitor therapy in squamous cell carcinoma xenografts. Head & Neck 2008; 30: 1-10.

[40] Zannetti A, Iommelli F, Speranza A, Salvatore M, del Vecchio S. 3“-deoxy-3-”18F-fluorothymidine PET/CT to guide therapy with epidermal growth factor receptor antagonists and Bcl-xL inhibitors in non-small cell lung cancer. J Nucl Med 2012; 53: 1-8.

[41] Vergez S, Delord JP, Thomas F, Rochaix P, Caselles O, Filleron T, Brillouet S, Canal P, Courbon F, Allal BC. Preclinical and Clinical Evidence that Deoxy-2-[18F]fluoro-D-glucose Positron Emission Tomography with Computed Tomography Is a Reliable Tool for the Detection of Early Molecular Responses to Erlotinib in Head and Neck Cancer. Clin Cancer Res 2010; 16: 4434-45.

[42] Solit DB, Santos E, Pratilas CA, Lobo J, Moroz M, Cai S, Blasberg R, Sebolt-Leopold J, Larson S, Rosen N. 3“-deoxy-3-”[18F]fluorothymidine positron emission tomography is a sensitive method for imaging the response of BRAF-dependent tumors to MEK inhibition. Cancer Res 2007; 67: 11463-9.

[43] Tegnebratt T, Lu L, Lee L, Meresse V, Tessier J, Ishii N, Harada N, Pisa P, Stone-El S, Stone-Elander S. [18 F]FDG-PET imaging is an early non-invasive pharmacodynamic biomarker for a first-in-class dual MEK/Raf inhibitor, RO5126766 (CH5126766), in preclinical xenograft models. EJNMMI Res 2013; 3: 67.

[44] Takeuchi S, Zhao S, Kuge Y, Zhao Y, Nishijima K, Hatano T, Shimizu Y, Kinoshita I, Tamaki N, Dosaka-Akita H. 18F-Fluorothymidine PET/CT as an early predictor of tumor response to treatment with cetuximab in human lung cancer xenografts. Oncol Rep 2011 ; 26: 725-30.

[45] Manning HC, Merchant NB, Foutch AC, Virostko JM, Wyatt SK, Shah C, McKinley ET, Xie J, Mutic NJ, Washington MK, LaFleur B, Tantawy MN, Peterson TE, Ansari MS, Baldwin RM, Rothenberg ML, Bornhop DJ, Gore JC, Coffey RJ, Manning HC, Merchant NB, Foutch AC, Virostko JM, Wyatt SK, Shah C, McKinley ET, Xie J, Mutic NJ, Washington MK, LaFleur B, Tantawy MN, Peterson TE, Ansari MS, Baldwin RM, Rothenberg ML, Bornhop DJ, Gore JC, Coffey RJ. Molecular Imaging of Therapeutic Response to Epidermal Growth Factor Receptor Blockade in Colorectal Cancer. Clin Cancer Res 2008; 14: 7413-22.

[46] Shah C, Miller TW, Wyatt SK, McKinley ET, Olivares MG, Sanchez V, Nolting DD, Buck JR, Zhao P, Ansari MS, Baldwin RM, Gore JC, Schiff R, Arteaga CL, Manning HC. Imaging Biomarkers Predict Response to Anti-HER2 (ErbB2) Therapy in Preclinical Models of Breast Cancer. Clin Cancer Res 2009; 15: 4712-21.

[47] McLarty K, Fasih A, Scollard DA, Done SJ, Vines DC, Green DE, Costantini DL, Reilly RM. 18F-FDG small-animal PET/CT differentiates trastuzumab-responsive from unresponsive human breast cancer xenografts in athymic mice. J Nucl Med 2009; 50: 1848-56.

[48] Dorow DS, Cullinane C, Conus N, Roselt P, Binns D, McCarthy TJ, McArthur GA, Hicks RJ. Multi-tracer small animal PET imaging of the tumour response to the novel pan-Erb-B inhibitor CI-1033. EurJ Nucl Med MolImaging 2006; 33: 1-12.

[49] Janjigian YY, Viola-Villegas N, Holland JP, Divilov V, Carlin SD, Gomes-Dagama EM, Chiosis G, Carbonetti G, de Stanchina E, Lewis JS. Monitoring Afatinib Treatment in HER2-Positive Gastric Cancer with 18F-FDG and 89Zr-Trastuzumab PET. J Nucl Med 2013; 54: 936-43.

[50] Cullinane C, Dorow DS, Kansara M, Conus N, Binns D, Hicks RJ, Ashman LK, McArthur GA, Thomas DM, Cullinane C. An In vivo Tumor Model Exploiting Metabolic Response as a Biomarker for Targeted Drug Development. Cancer Res 2005; 65: 1-5.

[51] Prenen H, Deroose C, Vermaelen P, Sciot R, Debiec-Rychter M, Stroobants S, Mortelmans L, Schöffski P, van Oosterom A. Establishment of a mouse gastrointestinal stromal tumour model and evaluation of response to imatinib by small animal positron emission tomography. Anticancer Res 2006; 26: 1247-52.

[52] Treglia G, Mirk P, Stefanelli A, Rufini V, Giordano A, Bonomo L. 18F-Fluorodeoxyglucose positron emission tomography in evaluating treatment response to imatinib or other drugs in gastrointestinal stromal tumors: a systematic review. Clin Imaging 2012; 36: 167-75.

[53] Stroobants S, Goeminne J, Seegers M, Dimitrijevic S, Dupont P, Nuyts J, Martens M, van den Borne B, Cole P, Sciot R, Dumez H, Silberman S, Mortelmans L, van Oosterom A. 18FDG-Positron emission tomography for the early prediction of response in advanced soft tissue sarcoma treated with imatinib mesylate (Glivec). Eur J Cancer 2003; 39: 2012-20.

[54] Rex K, Lewis XZ, Gobalakrishnan S, Glaus C, Silva MD, Radinsky R, Burgess TL, Gambhir SS, Coxon A. Evaluation of the antitumor effects of rilotumumab by PET imaging in a U-87 MG mouse xenograft model 2013; 40: 458-63.

[55] Cullinane C, Dorow DS, Jackson S, Solomon B, Bogatyreva E, Binns D, Young R, Arango ME, Christensen JG, McArthur GA, Hicks RJ. Differential (18)F-FDG and 3"-deoxy-3-"(18) F-fluorothymidine PET responses to pharmacologic inhibition of the c-MET receptor in preclinical tumor models. J Nucl Med 2011; 52: 1261-7.

[56] Wiehr S, Ahsen von O, Röse L, Mueller A, Mannheim JG, Honndorf V, Kukuk D, Reischl G, Pichler BJ. Preclinical evaluation of a novel c-Met inhibitor in a gastric cancer xenograft model using small animal PET. Mol Imaging Biol 2013; 15: 203-11.

[57] Tseng JR, Kang KW, Dandekar M, Yaghoubi S, Lee JH, Christensen JG, Muir S, Vincent PW, Michaud NR, Gambhir SS. Preclinical efficacy of the c-Met inhibitor CE-355621 in a U87 MG mouse xenograft model evaluated by 18F-FDG small-animal PET. J Nucl Med 2008; 49: 129-34.

[58] Keen HG, Ricketts SA, Maynard J, Logie A, Odedra R, Shannon AM, Wedge SR, Guichard SM. Examining changes in [18 F]FDG and [18 F]FLT uptake in U87-MG glioma xenografts as early response biomarkers to treatment with the dual mTOR1/2 inhibitor AZD8055. Mol Imaging Biol 2014; 16: 421-30.

[59] Li Z, Graf N, Herrmann K, Jünger A, Aichler M, Feuchtinger A, Baumgart A, Walch A, Peschel C, Schwaiger M, Buck A, Keller U, Dechow T. FLT-PET is superior to FDG-PET for very early response prediction in NPM-ALK-positive lymphoma treated with targeted therapy. Cancer Res 2012; 72: 1-12.

[60] Thomas GV, Tran C, Mellinghoff IK, Welsbie DS, Chan E, Fueger B, Czernin J, Sawyers CL. Hypoxia-inducible factor determines sensitivity to inhibitors of mTOR in kidney cancer. Nat Med 2005; 12: 122-127.

[61] Aide N, Kinross K, Cullinane C, Roselt P, Waldeck K, Neels O, Dorow D, McArthur G, Hicks RJ. 18F-FLT PET as a Surrogate Marker of Drug Efficacy During mTOR Inhibition by Everolimus in a Preclinical Cisplatin-Resistant Ovarian Tumor Model. J Nucl Med 2010 ; 51: 1559-64.

[62] Saint-Hubert MD, Devos E, Ibrahimi A, Debyser Z, Mortelmans L, Mottaghy FM. Bioluminescence imaging of therapy response does not correlate with FDG-PET response in a mouse model of Burkitt lymphoma. Am J Nucl Med Mol Imaging 2012; 2: 353-61.

[63] Saint-Hubert MD, Brepoels L, Devos E, Vermaelen P, Groot TD, Tousseyn T, Mortelmans L, Mottaghy FM. Molecular imaging of therapy response with (18)F-FLT and (18)F-FDG following cyclophosphamide and mTOR inhibition. Am J Nucl Med Mol Imaging 2012; 2: 110-21.

[64] Brepoels L, Stroobants S, Verhoef G, De Groot T, Mortelmans L, De Wolf-Peeters C, De Wolf-Peeters C. 18F-FDG and 18F-FLT Uptake Early After Cyclophosphamide and mTOR Inhibition in an Experimental Lymphoma Model. J Nucl Med 2009; 50: 1102-9.

[65] Wei LH, Su H, Hildebrandt IJ, Phelps ME, Czernin J, Weber WA. Changes in tumor metabolism as readout for Mammalian target of rapamycin kinase inhibition by rapamycin in glioblastoma. Clin Cancer Res 2008; 14: 3416-26.

[66] Honer M, Ebenhan T, Allegrini PR, Ametamey SM, Becquet M, Cannet C, Lane HA, O'Reilly TM, Schubiger PA, Sticker-Jantscheff M, Stumm M, McSheehy PM. Anti-Angiogenic/Vascular Effects of the mTOR Inhibitor Everolimus Are Not Detectable by FDG/FLT-PET. Transl Oncol 2010; 3: 1-14.

[67] Cejka D, Kuntner C, Preusser M, Fritzer-Szekeres M, Fueger BJ, Strommer S, Werzowa J, Fuereder T, Wanek T, Zsebedics M, Mueller M, Langer O, Wacheck V. FDG uptake is a surrogate marker for defining the optimal biological dose of the mTOR inhibitor everolimus in vivo. Br J Cancer 2009; 100: 1-7.

[68] Johnbeck CB, Munk Jensen M, Haagen Nielsen C, Fisker Hag AM, Knigge U, Kjaer A. 18F-FDG and 18F-FLT-PET imaging for monitoring everolimus effect on tumor-growth in neuroendocrine tumors: studies in human tumor xenografts in mice. PLoS One 2014; 9: e91387.

[69] Maynard J, Ricketts SA, Gendrin C, Dudley P, Davies BR. 2-Deoxy-2-[18F]fluoro-D-glucose positron emission tomography demonstrates target inhibition with the potential to predict anti-tumour activity following treatment with the AKT inhibitor AZD5363. Mol Imaging Biol 2013; 15: 476-85.

[70] Fuereder T, Wanek T, Pflegerl P, Jaeger-Lansky A, Hoeflmayer D, Strommer S, Kuntner C, Wrba F, Werzowa J, Hejna M, Müller M, Langer O, Wacheck V. Gastric cancer growth control by BEZ235 in vivo does not correlate with PI3K/mTOR target inhibition but with [18F]FLT uptake. Clin Cancer Res 2011; 17: 1-12.

[71] Cawthorne C, Burrows N, Gieling RG, Morrow CJ, Forster D, Gregory J, Radigois M, Smigova A, Babur M, Simpson K, Hodgkinson C, Brown G, McMahon A, Dive C, Hiscock D, Wilson I, Williams KJ. [18F]-FLT Positron Emission Tomography can be used to image the response of sensitive tumors to PI3-Kinase inhibition with the novel agent GDC-0941. Mol Cancer Ther 2013; 12: 819-28.

[72] Haagensen EJ, Thomas HD, Wilson I, Harnor SJ, Payne SL, Rennison T, Smith KM, Maxwell RJ, Newell DR. The enhanced in vivo activity of the combination of a MEK and a PI3K inhibitor correlates with [18F]-FLT PET in human colorectal cancer xenograft tumour-bearing mice. PLoS One 2013; 8: e81763.

[73] Vasudev NS, Reynolds AR. Anti-angiogenic therapy for cancer: current progress, unresolved questions and future directions. Angiogenesis 2014; 17: 471-494.

[74] Sandler A, Gray R, Perry MC, Brahmer J, Schiller JH, Dowlati A, Lilenbaum R, Johnson DH. Paclitaxel-carboplatin alone or with bevacizumab for non-small-cell lung cancer. N Engl J Med 2006; 355: 2542-50.

[75] Jain RK. Normalizing tumor microenvironment to treat cancer: bench to bedside to biomarkers. J Clin Oncol 2013; 31: 2205-18.

[76] Meier R, Braren R, Kosanke Y, Bussemer J, Neff F, Wildgruber M, Schwarzenböck S, Frank A, Haller B, Hohlbaum AM, Schwaiger M, Gille H, Rummeny EJ, Beer AJ. Multimodality multiparametric imaging of early tumor response to a novel antiangiogenic therapy based on anticalins. PLoS One 2014; 9: e94972.

[77] Kristian A, Revheim ME, Qu H, Mælandsmo GM, Engebråten O, Seierstad T, Malinen E. Dynamic (18)F-FDG-PET for monitoring treatment effect following anti-angiogenic therapy in triple-negative breast cancer xenografts. Acta Oncol 2013; 52: 1566-72.

[78] Corroyer-Dulmont A, Pérès EA, Petit E, Guillamo J-S, Varoqueaux N, Roussel S, Toutain J, Divoux D, MacKenzie ET, Delamare J, Ibazizène M, Lecocq M, Jacobs AH, Barré L, Bernaudin M, Valable S. Detection of glioblastoma response to temozolomide combined with bevacizumab based on μMRI and μPET imaging reveals [18F]-fluoro-L-thymidine as an early and robust predictive marker for treatment efficacy. Neuro Oncol 2013; 15: 41-56.

[79] Kim TJ, Ravoori M, Landen CN, Kamat AA, Han LY, Lu C, Lin YG, Merritt WM, Jennings N, Spannuth WA, Langley R, Gershenson DM, Coleman RL, Kundra V, Sood AK. Antitumor and antivascular effects of AVE8062 in ovarian carcinoma. Cancer Res 2007; 67: 9337-45.

[80] Moonshi SS, Bejot R, Atcha Z, Vijayaragavan V, Bhakoo KK, Goggi JL. A comparison of PET imaging agents for the assessment of therapy efficacy in a rodent model of glioma. Am J Nucl Med Mol Imaging 2013; 3: 397-407.

[81] Bao X, Wang MW, Zhang YP, Zhang YJ. Early monitoring antiangiogenesis treatment response of Sunitinib in U87MG Tumor Xenograft by (18)F-FLT MicroPET/CT imaging. Biomed Res Int 2014; 2014: 218578.

[82] Li Z, Herrmann K, Pirsig S, Philipp-Abbrederis K, Henninger M, Aichler M, Feuchtinger A, Walch A, Beer AJ, Ringshausen I, Pomykala KL, Scheidhauer K, Schwaiger M, Keller U, Buck AK. Molecular imaging for early prediction of

response to Sorafenib treatment in sarcoma. Am J Nucl Med Mol Imaging 2013; 4: 70-9.
[83] Karroum O, Mignion L, Kengen J, Karmani L, Levêque P, Danhier P, Magat J, Bol A, Labar D, Grégoire V, Bouzin C, Feron O, Gallez B, Jordan BF. Multimodal imaging of tumor response to sorafenib combined with radiation therapy: comparison between diffusion-weighted MRI, choline spectroscopy and 18F-FLT PET imaging. Contrast Media Mol Imaging 2013; 8: 274-80.
[84] Goggi JL, Bejot R, Moonshi SS, Bhakoo KK. Stratification of 18F-labeled PET imaging agents for the assessment of antiangiogenic therapy responses in tumors. J Nucl Med 2013; 54: 1630-6.
[85] Yang M, Gao H, Yan Y, Sun X, Chen K, Quan Q, Lang L, Kiesewetter D, Niu G, Chen X. PET imaging of early response to the tyrosine kinase inhibitor ZD4190. Eur J Nucl Med Mol Imaging 2011; 38: 1237-47.
[86] Leyton J, Smith G, Smith G, Lees M, Lees M, Perumal M, Nguyen QD, Nguyen QD, Aigbirhio FI, Aigbirhio FI, Golovko O, Golovko O, He Q, He Q, Workman P, Aboagye EO, Leyton J, Smith G, Lees M, Perumal M, Nguyen QD, Aigbirhio FI, Golovko O, He Q, Workman P, Aboagye EO. Noninvasive imaging of cell proliferation following mitogenic extracellular kinase inhibition by PD0325901. Mol Cancer Ther 2008; 7: 1-11.
[87] McKinley ET, Smith RA, Zhao P, Fu A, Saleh SA, Uddin MI, Washington MK, Coffey RJ, Manning HC. 3"-Deoxy-3-"18F-fluorothymidine PET predicts response to (V600E)BRAF-targeted therapy in preclinical models of colorectal cancer. J Nucl Med 2013; 54: 424-30.
[88] Habibollahi P, van den Berg NS, Kuruppu D, Loda M, Mahmood U. Metformin--an adjunct antineoplastic therapy--divergently modulates tumor metabolism and proliferation, interfering with early response prediction by 18F-FDG PET imaging. J Nucl Med 2013; 54: 252-8.
[89] Jensen MM, Erichsen KD, Johnbeck CB, Björkling F, Madsen J, Bzorek M, Jensen PB, Højgaard L, Sehested M, Kjær A. [18F]FLT and [18F]FDG PET for non-invasive treatment monitoring of the nicotinamide phosphoribosyltransferase inhibitor APO866 in human xenografts. PLoS One 2013; 8: e53410.
[90] Jensen MM, Erichsen KD, Björkling F, Madsen J, Jensen PB, Højgaard L, Sehested M, Kjær A. Early detection of response to experimental chemotherapeutic Top216 with [18F]FLT and [18F]FDG PET in human ovary cancer xenografts in mice. PLoS One 2010; 5: 1-9.
[91] Jensen MM, Erichsen KD, Björkling F, Madsen J, Jensen PB, Sehested M, Højgaard L, Kjær A. [18F]FLT PET for non-invasive assessment of tumor sensitivity to chemotherapy: studies with experimental chemotherapy TP202377 in human cancer xenografts in mice. PLoS One 2012; 7: e50618.
[92] Stelter L, Fuchs S, Jungbluth AA, Ritter G, Longo VA, Zanzonico P, Raschzok N, Sauer IM, Bomalaski JS, Larson SM. Evaluation of Arginine Deiminase Treatment in Melanoma Xenografts Using (18)F-FLT PET. Mol Imaging Biol 2013; 15: 768-75.
[93] Moroz MA, Moroz MA, Kochetkov T, Kochetkov T, Cai S, Wu J, Wu J, Shamis M, Shamis M, Nair J, Nair J, de Stanchina E, Serganova I, Serganova I, Schwartz GK, Schwartz GK, Banerjee D, Banerjee D, Bertino JR, Bertino JR, Blasberg RG, Blasberg RG, Moroz MA, Kochetkov T, Cai S, Wu J, Shamis M, Nair J, de Stanchina E, Serganova I, Schwartz GK, Banerjee D, Bertino JR, Blasberg RG. Imaging Colon Cancer Response Following Treatment with AZD1152: A Preclinical Analysis of [18F] Fluoro-2-deoxyglucose and 3"-deoxy-3-"[18F] Fluorothymidine Imaging. Clinical Cancer Research 2011; 17: 1-13.
[94] Cullinane C, Waldeck KL, Binns D, Bogatyreva E, Bradley DP, de Jong R, McArthur GA, Hicks RJ. Preclinical FLT-PET and FDG-PET imaging of tumor response to the multi-targeted Aurora B kinase inhibitor, TAK-901. Nucl Med Biol 2014; 41: 148-54.
[95] Chan F, Sun C, Perumal M, Nguyen QD, Bavetsias V, McDonald E, Martins V, Wilsher NE, Raynaud FI, Valenti M, Eccles S, Poele RT, Workman P, Aboagye EO, Linardopoulos S. Mechanism of action of the Aurora kinase inhibitor CCT129202 and in vivo quantification of biological activity. Mol Cancer Ther 2007; 6: 3147-3157.
[96] Smith-Jones PM, Solit D, Afroze F, Rosen N, Larson SM. Early tumor response to Hsp90 therapy using HER2 PET: comparison with 18F-FDG PET. J Nucl Med 2006; 47: 1-4.
[97] Mudd SR, Holich KD, Voorbach MJ, Cole TB, Reuter DR, Tapang P, Bukofzer G, Chakravartty A, Donawho CK, Palma JP, Fox GB, Day M, Luo Y. Pharmacodynamic Evaluation of Irinotecan Therapy by FDG and FLT PET/CT Imaging in a Colorectal Cancer Xenograft Model. Mol Imaging Biol 2012; 14: 617-24.
[98] Na YS, Jung KA, Kim SM, Hong YS, Ryu MH, Jang SJ, Moon DH, Cho DH, Kim JC, Lee JS, Kim TW. The histone deacetylase inhibitor PXD101 increases the efficacy of irinotecan in in vitro and in vivo colon cancer models. Cancer Chemother Pharmacol 2011; 68: 389-98.
[99] Chan PC, Wu CY, Chou LS, Ho CH, Chang CW, Chiou SH, Lin WJ, Chen FD, Chang CA, Hwang JJ, Liu RS, Wang HE. Monitoring Tumor Response After Histone Deacetylase Inhibi-

tor Treatment Using 3"-Deoxy-3-"[(18)F]-fluorothymidine PET. Mol Imaging Biol 2015; 17: 394-402.

[100] Jensen MM, Erichsen KD, Johnbeck CB, Björkling F, Madsen J, Jensen PB, Sehested M, Højgaard L, Kjær A. [18F]FDG and [18F]FLT positron emission tomography imaging following treatment with belinostat in human ovary cancer xenografts in mice. BMC Cancer 2013; 13: 168.

[101] Oyama N, Hasegawa Y, Kiyono Y, Kobayashi M, Fujibayashi Y, Ponde DE, Dence C, Welch MJ, Yokoyama O. Early response assessment in prostate carcinoma by ^{18}F-fluorothymidine following anticancer therapy with docetaxel using preclinical tumour models. Eur J Nucl Med Mol Imaging 2011; 38: 81-9.

[102] Sun X, Yan Y, Liu S, Cao Q, Yang M, Neamati N, Shen B, Niu G, Chen X. 18F-FPPRGD2 and 18F-FDG PET of response to Abraxane therapy. J Nucl Med 2011; 52: 140-6.

[103] Lee SJ, Kang HY, Kim SY, Chung JH, Oh SJ, Ryu JS, Kim SB, Kang JS, Park SK, Kim HM, Kim MH, Moon DH. Early assessment of tumor response to JAC106, an anti-tubulin agent, by 3"-deoxy-3-"[^{18}F]fluorothymidine in preclinical tumor models. Eur J Nucl Med Mol Imaging 2011; 38: 1436-48.

[104] Ebenhan T, Honer M, Ametamey SM, Schubiger PA, Becquet M, Ferretti S, Cannet C, Rausch M, McSheehy PM. Comparison of [18F]-tracers in various experimental tumor models by PET imaging and identification of an early response biomarker for the novel microtubule stabilizer patupilone. Mol Imaging Biol 2009; 11: 1-14.

[105] Jensen MM, Erichsen KD, Björkling F, Madsen J, Jensen PB, Sehested M, Højgaard L, Kjær A. Imaging of treatment response to the combination of carboplatin and paclitaxel in human ovarian cancer xenograft tumors in mice using FDG and FLT PET. PLoS One 2013; 8: e85126.

[106] Viel T, Schelhaas S, Wagner S, Wachsmuth L, Schwegmann K, Kuhlmann M, Faber C, Kopka K, Schäfers M, Jacobs AH. Early assessment of the efficacy of temozolomide chemotherapy in experimental glioblastoma using [18F]FLT-PET imaging. PLoS One 2013; 8: e67911.

[107] Aide N, Poulain L, Briand M, Dutoit S, Allouche S, Labiche A, Do Ngo-Van A, Nataf V, Batalla A, Gauduchon P, Talbot JN, Montravers F. Early evaluation of the effects of chemotherapy with longitudinal FDG small-animal PET in human testicular cancer xenografts: early flare response does not reflect refractory disease. Eur J Nucl Med Mol Imaging 2009; 36: 396-405.

[108] Perumal M, Stronach EA, Gabra H, Aboagye EO. Evaluation of 2-deoxy-2-[18F]fluoro-D-glucose- and 3"-deoxy-3-"[18F]fluorothymidine-positron emission tomography as biomarkers of therapy response in platinum-resistant ovarian cancer. Mol Imaging Biol 2012; 14: 753-61.

[109] Perumal M, Pillai RG, Barthel H, Leyton J, Latigo JR, Forster M, Mitchell F, Jackman AL, Aboagye EO. Redistribution of nucleoside transporters to the cell membrane provides a novel approach for imaging thymidylate synthase inhibition by positron emission tomography. Cancer Res 2006; 66: 8558-64.

[110] Ki Hong Il, Kim SY, Chung JH, Lee SJ, Oh SJ, Lee SJ, Oh J, Ryu JS, Kim TW, Kim DY, Moon DH. 3"-Deoxy-3-"[18F]fluorothymidine positron emission tomography imaging of thymidine kinase 1 activity after 5-fluorouracil treatment in a mouse tumor model. Anticancer Res 2014; 34: 759-66.

[111] Lee SJ, Kim SY, Chung JH, Oh SJ, Ryu JS, Hong YS, Kim TW, Moon DH. Induction of thymidine kinase 1 after 5-fluorouracil as a mechanism for 3'-deoxy-3'-[18F]fluorothymidine flare. Biochem Pharmacol 2010; 80: 1528-1536.

[112] Aliaga A, Rousseau JA, Cadorette J, Croteau E, van Lier JE, Lecomte R, Bénard F. A small animal positron emission tomography study of the effect of chemotherapy and hormonal therapy on the uptake of 2-deoxy-2-[F-18]fluoro-D-glucose in murine models of breast cancer. Mol Imaging Biol 2007; 9: 144-50.

[113] Shah N, Zhai G, Knowles JA, Stockard CR, Grizzle WE, Fineberg N, Zhou T, Zinn KR, Rosenthal EL, Kim H. (18)F-FDG PET/CT imaging detects therapy efficacy of anti-EMMPRIN antibody and gemcitabine in orthotopic pancreatic tumor xenografts. Mol Imaging Biol 2012; 14: 237-44.

[114] Lee WC, Chang CH, Ho CL, Chen LC, Wu YH, Chen JT, Wang YL, Lee TW. Early detection of tumor response by FLT/microPET Imaging in a C26 murine colon carcinoma solid tumor animal model. J Biomed Biotechnol 2011; 2011: 535902.

[115] Zhang F, Zhu L, Liu G, Hida N, Lu G, Eden HS, Niu G, Chen X. Multimodality imaging of tumor response to doxil. Theranostics 2011; 1: 302-9.

[116] Graf N, Herrmann K, den Hollander J, Fend F, Schuster T, Wester HJ, Senekowitsch-Schmidtke R, Büschenfelde CM, Peschel C, Schwaiger M, Dechow T, Buck AK. Imaging Proliferation to Monitor Early Response of Lymphoma to Cytotoxic Treatment. Mol Imaging Biol 2008; 10: 349-55.

[117] Graf N, Herrmann K, Numberger B, Zwisler D, Aichler M, Feuchtinger A, Schuster T, Wester HJ, Senekowitsch-Schmidtke R, Peschel C, Schwaiger M, Keller U, Dechow T, Buck AK. [(18)F]FLT is superior to [(18)F]FDG for predicting early response to antiproliferative treat-

ment in high-grade lymphoma in a dose-dependent manner. Eur J Nucl Med Mol Imaging 2013; 40: 34-43.

[118] Zhang Y, Saylor M, Wen S, Silva MD, Rolfe M, Bolen J, Muir C, Reimer C, Chandra S. Longitudinally quantitative 2-deoxy-2-[18F]fluoro-D-glucose micro positron emission tomography imaging for efficacy of new anticancer drugs: a case study with bortezomib in prostate cancer murine model. Mol Imaging Biol 2006; 8: 300-8.

[119] Jensen MM, Erichsen KD, Bjorkling F, Madsen J, Jensen PB, Hojgaard L, Sehested M, Kjaer A. Early detection of response to experimental chemotherapeutic Top216 with [18F]FLT and [18F]FDG PET in human ovary cancer xenografts in mice. PLoS One 2010; 5: e12965.

[120] Pardo OE, Latigo J, Jeffery RE, Nye E, Poulsom R, Spencer-Dene B, Lemoine NR, Stamp GW, Aboagye EO, Seckl MJ, Pardo OE, Latigo J, Jeffery RE, Nye E, Poulsom R, Spencer-Dene B, Lemoine NR, Stamp GW, Aboagye EO, Seckl MJ. The Fibroblast Growth Factor Receptor Inhibitor PD173074 Blocks Small Cell Lung Cancer Growth In vitro and In vivo. Cancer Res 2009; 69: 1-8.